In presenting the dissertation as a partial fulfillment of the requirements for an advanced degree from the Georgia Institute of Technology, I agree that the Library of the Institute shall make it available for inspection and circulation in accordance with its regulations governing materials of this type. I agree that permission to copy from, or to publish from, this dissertation may be granted by the professor under whose direction it was written, or, in his absence, by the Dean of the Graduate Division when such copying or publication is solely for scholarly purposes and does not involve potential financial gain. It is understood that any copying from, or publication of, this dissertation which involves potential financial gain will not be allowed without written permission.

7/25/68

# PROPERTIES, LIMITATIONS, AND APPLICATIONS OF THE RADAR AMBIGUITY FUNCTION

A THESIS

Presented to

The Faculty of the Graduate Division

by

William Milton Brown, Jr.

In Partial Fulfillment

of the Requirements for the Degree

Master of Science in Electrical Engineering

Georgia Institute of Technology

April, 1969

PROPERTIES, LIMITATIONS, AND APPLICATIONS

OF THE RADAR AMBIGUITY FUNCTION

Approved:

Date approved by Chairman: 4-17-69

# ACKNOWLEDGMENTS

I wish to thank Dr. R. H. Pettit for suggesting this problem and for his patience while awaiting its completion. I also wish to thank Dr. H. A. Ecker and Dr. A. M. Bush for serving on my committee and for their numerous helpful suggestions.

TABLE OF CONTENTS

# LIST OF ILLUSTRATIONS

## SUMMARY

The radar ambiguity function is studied with emphasis on its properties, limitations, and applications. The properties form a set of conditions which all ambiguity functions must obey and which are useful in predicting the distribution of the ambiguity function in range and Doppler. The ambiguity function has two types of limitations. First the ambiguity function is a valid representation of the matched filter output only when

(1) The modulation bandwidth of the transmitted signal is small compared with the carrier frequency.

(2) The effect of a moving target on the transmitted waveform can be represented by a simple frequency shift.

(3) The velocity of the target, $V_r$, must satisfy the restriction

$$V_r << (c/2)(1/BT_t)$$

where c is the speed of light, B is the bandwidth of the transmitted waveform, and $T_t$ is the total time duration of the waveform.

(4) The received waveform is assumed to be reflected from a non-distributed point target.

Secondly, the ambiguity function has two resolution limitations invariant to the selected waveform. The minimum resolution cell in

a uniformly dense target environment has an area of one and the maximum clear area which can surround the ambiguity origin has a value of one.

The ambiguity function is used to evaluate the resolution, accuracy and ambiguity of some typical waveforms. A waveform with high resolution in both Doppler and range is designed and some amplitude weighting techniques are demonstrated to greatly lower the ambiguity sidelobe level of this ambiguity function.

# CHAPTER I

## INTRODUCTION

Since radars first came into use, their function has been to measure a target's position or speed. For some time during the early days of radar it was believed that simultaneous measurement of velocity and position of a target was impossible. Arguments were advanced that good range resolution necessitated a short time duration waveform and good velocity resolution required relatively longer time durations. Peak power limitations caused designers to feel that range resolution had a practical limit, because a long pulse, incompatible with good range resolution, was usually required for an acceptable signal-to-noise ratio at the receiver for detection.

In 1953, P. M. Woodward wrote a monograph which introduced the radar ambiguity function (1). Woodward showed that the resolution cell of a radar was inversely proportional to a "time-bandwidth" product of the radar signal. Therefore, a long pulse could have good range resolution if modulation was used to increase the bandwidth of the pulse. Woodward's monograph stimulated interest in the design of waveforms optimum for the measurement of both range and velocity.

Early in the investigation of waveforms, it was found that there was not a unique solution to the problem of waveform selection. Waveforms suitable for a particular target environment were frequently not satisfactory when the characteristics of the environment changed

significantly. The ambiguity function is used to evaluate these different waveforms and test them for ambiguity, accuracy and resolution in a particular target environment.

A large amount of literature now exists on the ambiguity function. This literature (1) investigates the properties of the ambiguity function, (2) explains the limitations in its use, and (3) deals with specific applications of the ambiguity function to waveform selection.

The purpose of this paper is to draw from recent contributions in the literature and develop a unified treatment of the properties and limitations of the ambiguity function and to describe some of its applications to waveform selection.

The properties can be used to test a function in order to determine if it has the characteristics of an ambiguity function. The properties also have applications to graphing of the ambiguity function. For instance, the representation of the function in any two adjacent quadrants gives a complete description.

The limitations treated are of two types. The first type deals with the applicability of the ambiguity function as a representation of the squared magnitude of the matched filter output. This representation assumes that the transmitted signal can be represented in complex envelope form; that all radar echoes are from point targets; that the change in a waveform when it collides with a moving body can be represented by the Doppler shift; and that the effects of acceleration over the signal processing time are negligible.

The second type of limitation treated is a resolution limitation which arises directly as a result of the ambiguity functions' properties.

This limitation gives a constraint on the resolution capability of a radar in an extended target environment or the size of a confined environment for high resolution without ambiguity.

The applications were selected to exhibit the usefulness of the ambiguity function in designing waveforms for transmission. After summarizing recent work in clutter rejection applications, some specific waveforms are presented for selected target environments. The design of a pulse train is illustrated and some methods of eliminating undesired ambiguities associated with the pulse train are discussed.

# CHAPTER II

## PROPERTIES

Radar receivers must operate in an environment containing both clutter and thermal noise. Clutter noise consists of unwanted radar echoes and depends greatly on the interference from trees, land, man-made structures, or the sea surface in the particular target area. Thermal noise, a completely random phenomenon, has well-known statistics and has been carefully modeled. Lacking knowledge about the clutter distribution, the interference from Gaussian thermal noise can be minimized by optimum filtering.

Optimum radar receivers, operating in white noise, use a matched filter for predetection processing. This filter gives optimum predetection processing when the criterion of performance is maximizing the output signal-to-noise ratio (2). The matched filter is also an optimum filter for forming the likelihood ratio, which is important when a Bayes decision rule is used at the filter output (3). In addition, the matched filter satisfies the inverse probability criteria of Woodward's ideal receiver (4).

Note that the matched filter is an optimum filter for the class of all linear filters in white noise. Frequently noise from clutter does not have the same statistics as white noise, and hence a filter which is optimum in a clutter environment may not be matched. In addition, non-linear filters have not been considered and may have better characteristics.

The ambiguity function is defined as the squared magnitude of the matched filter envelope function, $\psi(\tau,\phi)$, derived in Appendix I, and is given by $|\psi(\tau,\phi)|^2$. The form of the function $\psi(\tau,\phi)$ is

$$\psi(\tau,\phi) = \int_{-\infty}^{\infty} u(t)u^*(t+\tau)e^{-j2\pi\phi t}dt, \tag{1}$$

where u(t) is the complex envelope of the transmitted waveform s(t) so that

$$s(t) = \mathrm{Re}\{u(t)e^{j2\pi f_o t}\}. \tag{2}$$

If the filter is not matched to the transmitted waveform, the ambiguity function is defined as the magnitude of convolution of the received waveform with the filter's impulse response normalized to a maximum height of one and squared. The symbol $\phi$ corresponds to the difference between the frequency of the received signal and the frequency at which the filter is matched. The symbol $\tau$ corresponds to the difference between the time delay of the received signal and the time delay where the filter maximizes the signal-to-noise ratio.

The function $\psi(\tau,\phi)$ is sometimes presented as

$$\psi(\tau,\phi) = \int_{-\infty}^{\infty} u(t)u^*(t-\tau)e^{j2\pi\phi t}dt. \tag{3}$$

Looking at Equation (1), if a change of variable is made such that

$$t' = t + \tau, \tag{4}$$

then

$$\psi(\tau,\phi) = \int_{-\infty}^{\infty} u(t'-\tau)u^{*}(t')e^{-j2\pi\phi(t'-\tau)}dt' \tag{5}$$

which becomes

$$\psi(\tau,\phi) = e^{j2\pi\phi\tau} \int_{-\infty}^{\infty} u(t'-\tau)u^{*}(t')e^{-j2\pi\phi t'}dt'. \tag{6}$$

The complex conjugate of Equation (6) is

$$\psi^{*}(\tau,\phi) = e^{-j2\pi\phi\tau} \int_{-\infty}^{\infty} u^{*}(t'-\tau)u(t')e^{j2\pi\phi t'}dt'. \tag{7}$$

Equation (7) differs from Equation (3) only by the phase factor $e^{-j2\pi\phi\tau}$. Since the quantity of interest is $|\psi(\tau,\phi)|^2$, both of the forms, Equations (1) and (3), yield an equivalent result.

An equivalent form of the ambiguity function exists when the complex modulation terms are represented in the frequency domain. By the application of Parseval's theorem, the envelope function then becomes

$$\psi(\tau,\phi) = \int_{-\infty}^{\infty} M^{*}(f)M(f+\phi)e^{-j2\pi ft}df, \tag{8}$$

where

$$M(f) = \int_{-\infty}^{\infty} u(t)e^{-j2\pi ft}dt. \tag{9}$$

## Properties Invariant to Waveform Selection

The study of the properties of the ambiguity function began almost immediately after the discovery of the application of the ambiguity function to radar waveform selection by Woodward (1). In 1958, W. M. Siebert presented a paper climaxing years of searching for the properties of the ambiguity function (5). Before these properties, first derived by Siebert, are discussed, another form of the ambiguity function will be derived which will facilitate the proof of some of the properties.

If we substitute

$$t' = t - \tau/2 \tag{10}$$

in Equation (3), then the matched filter envelope response becomes

$$\psi(\tau,\phi) = e^{j\pi\phi\tau}\int_{-\infty}^{\infty} u(t'+\tau/2)u^{*}(t'-\tau/2)e^{j2\pi\phi t'}dt'. \tag{11}$$

We may now define the envelope of Equation (11) by

$$\theta^{*}(\tau,\phi) = \int_{-\infty}^{\infty} u(t+\tau/2)u^{*}(t-\tau/2)e^{j2\pi\phi t}dt, \tag{12}$$

which can be represented with the complex envelope terms in the frequency domain by

$$\theta(\tau,\phi) = \int_{-\infty}^{\infty} M^{*}(f-\phi/2)M(f+\phi/2)e^{-j2\pi f\tau}df. \tag{13}$$

Since $\theta^*(\tau,\phi)$ and $\psi(\tau,\phi)$ differ only by the phase factor $e^{j\pi\phi\tau}$, a property which holds for $|\theta(\tau,\phi)|^2$ also holds for $|\psi(\tau,\phi)|^2$.

Some important properties of the ambiguity function which are not dependent on the selected waveform for transmission will now be presented.

Property I--Symmetry

The ambiguity function is symmetrical about the $(\tau,\phi)$ origin.

Beginning with the complex conjugate of Equation (12),

$$\theta(\tau,\phi) = \int_{-\infty}^{\infty} u^*(t+\tau/2)u(t-\tau/2)e^{-j2\pi\phi t}dt, \tag{14}$$

a new equation can be formed by replacing $(\tau,\phi)$ by $(-\tau,-\phi)$. Equation (14) becomes

$$\theta(-\tau,-\phi) = \int_{-\infty}^{\infty} u(t+\tau/2)u^*(t-\tau/2)e^{j2\pi\phi t}dt, \tag{15}$$

when this substitution is made. Likewise from Equation (12), a substitution of $(-\tau,-\phi)$ for $(\tau,\phi)$ yields

$$\theta^*(-\tau,-\phi) = \int_{-\infty}^{\infty} u^*(t+\tau/2)u(t-\tau/2)e^{-j2\pi\phi t}dt. \tag{16}$$

A comparison of Equations (14) and (16) shows that

$$\theta(\tau,\phi) = \theta^*(-\tau,-\phi). \tag{17}$$

The right-hand sides of Equations (14) and (15) are conjugates; therefore,

$$\theta^{*}(\tau,\phi) = \theta(-\tau,-\phi). \tag{18}$$

Equations (17) and (18) are multiplied together to give

$$|\theta(\tau,\phi)|^2 = |\theta(-\tau,-\phi)|^2, \tag{19}$$

and the proof of Property I is complete.

Property I is useful when the ambiguity function must be plotted. It allows the plotter to reflect each calculated point through the origin and thus plot two points with each calculation.

Property II--Position of the Greatest Magnitude

The magnitude of the ambiguity function at $\tau = \phi = 0$ is at least as large as its magnitude at any other point.

The Schwarz inequality is given by

$$[\int f^{*}(z)g(z)dz]^2 \leq \int f(z)f^{*}(z)dz \int g(z)g^{*}(z)dz. \tag{20}$$

The Schwarz inequality involving the ambiguity function with

$$u(t-\tau/2)e^{-j2\pi\phi t} = f^{*}(t) \tag{21}$$

and

$$u^{*}(t-\tau/2) = g(t) \tag{22}$$

is

$$|\theta(\tau,\phi)|^2 = \left|\int_{-\infty}^{\infty} u(t-\tau/2)u^{*}(t+\tau/2)e^{-j2\pi\phi t}dt\right|^2 \tag{23}$$

$$\leq \int_{-\infty}^{\infty} |u(t-\tau/2)|^2 dt \int_{-\infty}^{\infty} |u(t+\tau/2)|^2 dt.$$

A change of variables so that

$$t_1 = t - \tau/2 \tag{24}$$

and

$$t_2 = t + \tau/2 \tag{25}$$

can be made in both of the integrals on the right in Equation (23) to give the inequality

$$|\theta(\tau,\phi)|^2 \leq \int_{-\infty}^{\infty} |u(t_1)|^2 dt_1 \int_{-\infty}^{\infty} |u(t_2)|^2 dt_2. \tag{26}$$

However, both of the integrals on the right in Inequality (26) represent $\theta(0,0)$; therefore,

$$|\theta(\tau,\phi)|^2 \leq |\theta(0,0)|^2. \tag{27}$$

Property III--Time Scaling

If u(t) has a corresponding envelope function $\theta(\tau,\phi)$, then u(at) has a corresponding envelope function $\frac{1}{|a|}\theta(a\tau,\phi/a)$.

First, the envelope function, $\theta_1(\tau,\phi)$, for u(at) can be shown to equal

$$\int_{-\infty}^{\infty} u(a[t-\tau/2])u^*(a[t+\tau/2])e^{-j2\pi\phi t}dt. \tag{28}$$

If a substitution of variable is made

$$t' = at, \tag{29}$$

then for a > 0

$$\theta_1(\tau,\phi) = 1/a\int_{-\infty}^{\infty} u(t'-\frac{a\tau}{2})u^*(t'+\frac{at}{2})e^{-j2\pi(\phi/a)t'}dt', \tag{30}$$

and for a < 0

$$\theta_1(\tau,\phi) = -\frac{1}{a}\int_{-\infty}^{\infty} u(t'-\frac{a\tau}{2})u^*(t'+\frac{a\tau}{2})e^{-j2\pi(\phi/a)t'}dt', \tag{31}$$

which becomes for all a

$$\theta_1(\tau,\phi) = \frac{1}{|a|}\int_{-\infty}^{\infty} u(t'-\frac{a\tau}{2})u^*(t'+\frac{a\tau}{2})e^{-j2\pi(\phi/a)t'}dt'. \tag{32}$$

A comparison of Equations (32) and (14) shows that

$$\theta_1(\tau,\phi) = \frac{1}{|a|}\,\theta(a\tau,\phi/a). \tag{33}$$

The effects of time scaling on the complex envelope function u(t) can be seen directly in the ambiguity function by scaling the variable $\tau$ by a and the variable $\phi$ by 1/a. The constant $1/|a|$ preceding $\theta(a\tau,\phi/a)$ arises because the envelope function, u(t), has a different energy when the variable t is scaled. If the energy is again normalized to unity, the constant $1/|a|$ disappears.

Property IV--Maximum Value

The maximum value of the envelope function, $\psi(\tau,\phi)$, is equal to twice the energy content, 2E, of the received waveform where

$$E = \int_{-\infty}^{\infty} s^2(t)dt. \tag{34}$$

From Property II, the maximum value of $|\psi(\tau,\phi)|^2$ occurs at $\tau = \phi = 0$; therefore,

$$\psi(0,0) = \int_{-\infty}^{\infty} u(t)u^*(t)dt \tag{35}$$

which is recognized to be equal to 2E. Usually the maximum value of the ambiguity function is normalized to unity for purposes of comparing different waveforms.

Property V--Unitary Volume

The volume under the ambiguity function is equal to $|\psi(0,0)|^2$, which is normalized to unity.

The volume under the ambiguity function is given by

$$\int_{-\infty}^{\infty}\int_{-\infty}^{\infty}|\psi(\tau,\phi)|^2 d\tau d\phi = \tag{36}$$

$$\int_{-\infty}^{\infty}\int_{-\infty}^{\infty}\int_{-\infty}^{\infty}\int_{-\infty}^{\infty} u(t)u^*(t+\tau)M(f)M^*(f+\phi)e^{j2\pi(f\tau-\phi t)}dtdfd\tau d\phi.$$

The two Fourier transform pairs,

$$\int_{-\infty}^{\infty} u^*(t+\tau)e^{j2\pi f\tau}d\tau = e^{-j2\pi ft}M^*(f) \tag{37}$$

and

$$\int_{-\infty}^{\infty} M^*(f+\phi)e^{-j2\pi\phi t}d\phi = e^{j2\pi ft}u^*(t), \tag{38}$$

can be used to simplify Equation (36) to the form

$$\int_{-\infty}^{\infty}\int_{-\infty}^{\infty}|\psi(\tau,\phi)|^2 d\tau d\phi = \int_{-\infty}^{\infty}\int_{-\infty}^{\infty} u(t)u^*(t)M(f)M^*(f)dfdt. \tag{39}$$

The right-hand side of Equation (39) is recognized to be $|\psi(0,0)|^2$, and, therefore,

$$\int_{-\infty}^{\infty}\int_{-\infty}^{\infty}|\psi(\tau,\phi)|^2 d\tau d\phi = |\psi(0,0)|^2. \tag{40}$$

This result is often called the "law of the conservation of ambiguity." Regardless of the transmitted waveform, the total volume under the ambiguity function is one if the signal energy is normalized.

Property VI--Effects of Quadratic Phase in the Time Domain

If $\theta(\tau,\phi)$ corresponds to $u(t)$, then $\theta\left(\tau,\phi+\frac{K\tau}{\pi}\right)$ corresponds to $u(t)e^{jKt^2}$.

If $\phi + \frac{K\tau}{\pi}$ is substituted for $\phi$ in Equation (14), the result is

$$\theta\left(\tau,\phi+\frac{K\tau}{\pi}\right) = \int_{-\infty}^{\infty} u(t-\tau/2)u^*(t+\tau/2)e^{-j2\pi(\phi+K\tau/\pi)t}dt. \qquad (41)$$

The envelope function for $u(t)e^{jKt^2}$ is

$$\theta_1(\tau,\phi) = \int_{-\infty}^{\infty} u(t-\tau/2)u^*(t+\tau/2)e^{-j2Kt\tau}e^{-j2\pi\phi t}dt. \qquad (42)$$

By inspection, the right-hand sides of Equations (41) and (42) are identical, and

$$\theta_1(\tau,\phi) = \theta(\tau,\phi+K\tau/\pi), \qquad (43)$$

which proves Property VI.

Property VI is of considerable interest because linear frequency modulation is frequently used in radar systems. Using Property VI, the ambiguity function, $|\theta(\tau,\phi)|^2$, can be plotted for $u(t)$ and the ambiguity function for $u(t)e^{jKt^2}$ results from a change of variable.

Property VII--Effects of Quadratic Phase in the Frequency Domain

If $\theta(\tau,\phi)$ corresponds to $u(t)$, then $\theta\left(\tau+\frac{h\phi}{\pi},\phi\right)$ corresponds to $M(f)e^{jhf^2}$.

First, $\theta\left(\tau+\frac{h\phi}{\pi},\phi\right)$ can be formed by substituting $\tau+\frac{h\phi}{\pi}$ for $\tau$ in Equation (13), so that

$$\theta\left(\tau + \frac{h\phi}{\pi},\ \phi\right) = \int_{-\infty}^{\infty} M^{*}(f-\phi/2)M(f+\phi/2)e^{-j2hf\phi}e^{-j2\pi f\tau}df. \qquad (44)$$

The envelope function $\theta_1(\tau,\phi)$ which corresponds to $M(f)e^{jhf^2}$ is

$$\theta_1(\tau,\phi) = \int_{-\infty}^{\infty} M^{*}(f-\phi/2)M(f+\phi/2)e^{-j2hf\phi}e^{-j2\pi f\tau}df. \qquad (45)$$

By inspection

$$\theta_1(\tau,\phi) = \theta\left(\tau + \frac{h\phi}{\pi},\phi\right), \qquad (46)$$

and Property VII is proved.

Property VIII--Self-Transform Property

The ambiguity function has the transform property

$$|\psi(\nu,\sigma)|^2 = \int_{-\infty}^{\infty}\int_{-\infty}^{\infty} |\psi(\tau,\phi)|^2 e^{j2\pi(\phi\nu-\tau\sigma)}d\tau d\phi. \qquad (47)$$

Equation (47) can be rewritten using the complex envelope representation of the transmitted signal as

$$\int_{-\infty}^{\infty}\int_{-\infty}^{\infty} |\psi(\tau,\phi)|^2 e^{j2\pi(\phi\nu-\tau\sigma)}d\tau d\phi = \qquad (48)$$

$$\int_{-\infty}^{\infty}\int_{-\infty}^{\infty}\int_{-\infty}^{\infty}\int_{-\infty}^{\infty} u(t)u^{*}(t+\tau)M(f)M^{*}(f+\phi)e^{j2\pi\{(\nu-t)\phi-(\sigma-f)\tau\}}dtdfd\tau d\phi.$$

Substituting the transform pairs

$$\int_{-\infty}^{\infty} u^*(t+\tau)e^{-j2\pi\tau(\sigma-f)}d\tau = M^*(f-\sigma)e^{-j2\pi(f-\sigma)t} \tag{49}$$

and

$$\int_{-\infty}^{\infty} M^*(f+\phi)e^{j2\pi\phi(\nu-t)}d\phi = u^*(t-\nu)e^{j2\pi f(t-\nu)}, \tag{50}$$

and setting

$$p = t - \nu \tag{51}$$

and

$$q = f - \sigma, \tag{52}$$

Equation (48) becomes

$$\int_{-\infty}^{\infty}\int_{-\infty}^{\infty} |\psi(\tau,\phi)|^2 e^{j2\pi(\phi\nu-\tau\sigma)}d\tau d\phi = \tag{53}$$

$$\int_{-\infty}^{\infty}\int_{-\infty}^{\infty} u^*(p)u(p+\nu)M^*(q)M(q+\nu)e^{j2\pi(\sigma p-q\nu)}dpdq.$$

The right-hand side of Equation (53) is

$$\psi(\nu,\sigma)\psi^*(\nu,\sigma) = |\psi(\nu,\sigma)|^2; \tag{54}$$

therefore,

$$\int_{-\infty}^{\infty}\int_{-\infty}^{\infty} |\psi(\tau,\phi)|^2 e^{j2\pi(\phi\nu-\sigma\tau)}d\tau d\phi = |\psi(\nu,\sigma)|^2, \tag{54}$$

which proves Property VIII.

Certain ideally desired ambiguity functions can be shown to be nonexistent because they do not satisfy Property VIII.

Property IX--Volume Distribution

Two integral equations from Westerfield, presented without proof, help to explain the distribution of ambiguity volume (6). These equations are

$$\int_{-\infty}^{\infty}\{\int_{-\infty}^{\infty}|\psi(\tau,\phi)|^2 d\tau\}d\phi = \int_{-\infty}^{\infty}\{\int_{-\infty}^{\infty}|\psi(\tau,0)|^2 e^{-j2\pi\phi\tau} d\tau\}d\phi \qquad (56)$$

and

$$\int_{-\infty}^{\infty}\{\int_{-\infty}^{\infty}|\psi(\tau,\phi)|^2 d\phi\}d\tau = \int_{-\infty}^{\infty}\{\int_{-\infty}^{\infty}|\psi(0,\phi)|^2 e^{j2\pi\phi\tau} d\phi\}d\tau. \qquad (57)$$

Equation (56) shows that the distribution in volume of the ambiguity function for a given Doppler slot, $d\phi$, is given by the Fourier transform of the squared envelope of the ambiguity function on the delay axis. Equation (57) shows that the distribution of volume for a delay slot, $d\tau$, is given by the inverse Fourier transform of the squared envelope of the ambiguity function on the Doppler axis.

Property X--Rotational Invariance

An ambiguity function has rotational invariance if

$$\psi(\tau',\phi') = \psi(\tau,\phi) \qquad (58)$$

where

$$\begin{bmatrix} \tau' \\ \phi' \end{bmatrix} = \begin{bmatrix} \cos\theta & -\sin\theta \\ \sin\theta & \cos\theta \end{bmatrix} \begin{bmatrix} \tau \\ \phi \end{bmatrix}. \tag{59}$$

This rotational invariance property has been used by Klauder to develop a waveform whose ambiguity function has a central response peak which is sharply confined on both the Doppler and time delay axes (7).

Property XI--Taylor Expansion

The ambiguity function can be expanded around the $(\tau,\phi)$ origin in a two-dimensional Taylor's series to give Helstrom's ellipse (8). The expansion is

$$|\psi(\tau,\phi)|^2 = 1 - \tau^2\beta_o^2 - 2\tau\phi\alpha - \phi^2 t_o^2, \tag{60}$$

when truncated for terms of higher order (9). The term $\beta_o^2$ is the mean square frequency deviation of the transmitted signal given by

$$\beta_o^2 = \frac{(2\pi)^2 \int_{-\infty}^{\infty} f^2 |M(f)|^2 df}{\int_{-\infty}^{\infty} |M(f)|^2 df}. \tag{61}$$

The mean square time duration of the signal is given by

$$t_o^2 = \frac{(2\pi)^2 \int_{-\infty}^{\infty} t^2 |u(t)|^2 dt}{\int_{-\infty}^{\infty} |u(t)|^2 dt}, \tag{62}$$

and the "effective phase constant" of the signal is

$$\alpha = \frac{(2\pi)\int_{-\infty}^{\infty} t\theta'(t)|u(t)|^2 dt}{\int_{-\infty}^{\infty} |u(t)|^2 dt}, \tag{63}$$

where $\theta(t)$ is the angle of the complex envelope function $u(t)$,

$$u(t) = a(t)e^{j\theta(t)}, \tag{64}$$

and $a(t)$ is the magnitude. The "mean square frequency deviation," "mean square time duration," and the "effective phase constant" of the complex envelope $u(t)$ were first introduced by Gabor (10). However, Gabor used different scale factors from $(2\pi)$ on the integrals in Equations (61), (62), and (63). The use of the scale factor $(2\pi)$ produces a simpler expression for the measurement accuracy of a radar waveform.

If the ambiguity function is cut by a level plane at

$$|\psi(\tau,\phi)|^2 = \gamma^2 \tag{65}$$

then Equation (60) becomes

$$\beta_o^2\tau^2 + 2\tau\phi\alpha + t_o^2\phi^2 = 1 - \gamma^2. \tag{66}$$

Equation (66) always describes an ellipse and when the level plane is set such that

$$1 - \gamma^2 = 1/4, \tag{67}$$

Equation (66) describes Helstrom's ellipse. The ambiguity function is cut by a level plane at

$$|\psi(\tau,\phi)|^2 = 3/4, \tag{68}$$

because the resulting ellipse has an extent along the Doppler axis of $1/t_o$ and an extent along the delay axis of $1/\beta_o$. If $2E/N_o$ is equal to one, where $N_o$ is the single-sided noise power density, then $1/t_o$ represents the root mean square frequency error and $1/\beta_o$ represents the root mean square time error. Helstrom's ellipse, shown in Figure 1, gives an indication of the velocity and time delay measurement errors when $2E/N_o$ is equal to one, and allows comparisons between waveforms on the basis of errors in parameter estimation.

Property XII--Position of Maximum Value When u(t) Is Real

If u(t) is real, then for a constant $\tau$, $\tau = \tau_o$, the ambiguity function is largest when $\phi = 0$.

Since u(t) is real for all t, then

$$u^*(t+\tau_o) = u(t+\tau_o), \tag{69}$$

and

$$\psi(\tau_o,\phi) = \int_{-\infty}^{\infty} u(t)u(t+\tau_o)e^{-j2\pi\phi t}dt = r_o e^{i\theta}, \tag{70}$$

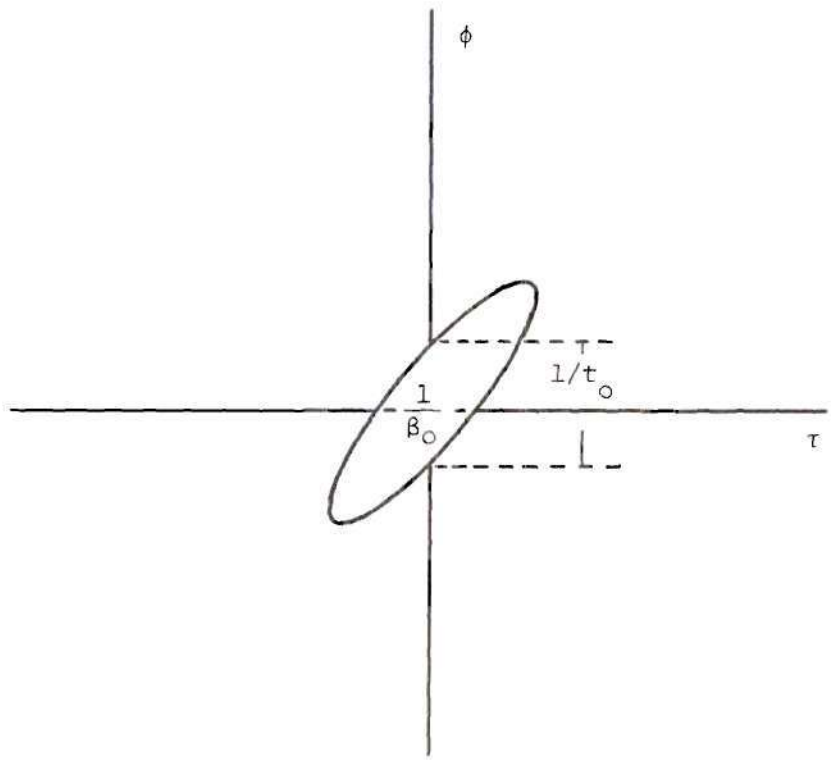


Figure 1. Helstrom's Ellipse. Cut Through the Central Peak of an Ambiguity Surface

where

$$r_o = |\psi(\tau_o,\phi)|. \tag{71}$$

Let

$$G_{\tau_o}(t) = u(t)u(t+\tau_o)e^{-j2\pi\phi t} \tag{72}$$

and

$$F_{\tau_o}(t) = u(t)u(t+\tau_o) = |G_{\tau_o}(t)|. \tag{73}$$

It follows that

$$\int_{-\infty}^{\infty} e^{-i\theta} G_{\tau_o}(t)dt = e^{-i\theta} \int_{-\infty}^{\infty} G_{\tau_o}(t)dt = r_o \tag{74}$$

and

$$r_o = \mathrm{Re}\{\int_{-\infty}^{\infty} e^{-i\theta} G_{\tau_o}(t)dt\} = \int_{-\infty}^{\infty} \mathrm{Re}\{e^{-i\theta} G_{\tau_o}(t)\}dt > 0; \tag{75}$$

but

$$\int_{-\infty}^{\infty} \mathrm{Re}\{e^{-i\theta} G_{\tau_o}(t)\}dt \le \int_{-\infty}^{\infty} |\mathrm{Re}[e^{-i\theta} G_{\tau_o}(t)]|dt \tag{76}$$

$$\le \int_{-\infty}^{\infty} |e^{-i\theta} G_{\tau_o}(t)|dt,$$

where Re{} denotes taking the real part of the function in brackets.

Equation (76) states that

$$r_o \le \int_{-\infty}^{\infty} F_{\tau_o}(t)dt, \tag{77}$$

or

$$|\psi(\tau_o,\phi)| \le \psi(\tau_o,0), \tag{78}$$

or

$$|\psi(\tau_o,\phi)|^2 \leq |\psi(\tau_o,0)|^2 \tag{79}$$

for any $\tau = \tau_o$.

# CHAPTER III

## LIMITATIONS IN THE USE OF THE AMBIGUITY FUNCTION AND RESOLUTION LIMITATIONS ARISING FROM ITS PROPERTIES

The limitations of the ambiguity function are a natural result of its properties and basically fall into two categories: (1) the ambiguity function cannot be applied to all waveforms because of the assumptions made in its derivation, and (2) resolution limitations arise as a result of the properties of the ambiguity function.

### Assumptions Made in the Derivation of the Ambiguity Function

First, let us look at the assumptions made in the derivation of the ambiguity function.

(1) Our complex envelope representation of the transmitted signal,

$$s(t) = \mathrm{Re}\{u(t)e^{j2\pi f_o t}\}, \tag{1}$$

is only valid when the modulation envelope of the radar signal has a narrow bandwidth when compared with the carrier frequency.

(2) The assumption was made that the time compression of a reflected waveform from a moving target could be accounted for by a single frequency shift. The time compression is

$$T - T' = T \frac{(1 - V_r/c)}{(1 + V_r/c)} \approx (1 - 2V_r/c)T \qquad (2)$$

where T - T' is the time duration of the compressed waveform with original duration T. The change in time duration is

$$T' = (T)(2V_r/c). \qquad (3)$$

The resolution of this waveform in range is given approximately by 1/B where B is the bandwidth of the waveform. If the effects of the time compression can be neglected then

$$T' << \frac{1}{B} \qquad (4)$$

or

$$(T) \frac{2V_r}{c} << \frac{1}{B} . \qquad (5)$$

Therefore,

$$V_r << \frac{c}{2T_t B} \qquad (6)$$

and the maximum velocity range over which the ambiguity function can be used is dependent on the time-bandwidth product of the transmitted signal.

(3) The ambiguity function assumes returns from point targets only.

(4) The approximation that the effects of acceleration can be ignored has also been made.

A good deal of research effort has been directed toward overcoming these limitations and some papers have reported successfully extending the ambiguity function to these excluded cases. Kelly and Wishner have extended the ambiguity function to include high-velocity targets, wideband signals, and the effects of acceleration (11). August Rihaczek has also generalized the form of the ambiguity function to bandwidths and velocities so large that the Doppler distortions of the modulation function must be considered (12). In addition, a form of the ambiguity function for extended bodies has been found by William Blau (13).

All of the above extensions of the ambiguity function result in a more complicated function, and generally the target environment and the transmitted waveform are such that none of these extensions applies. Because of the unextended ambiguity function's general applicability, it will be used to investigate and compare different waveforms.

## Resolution Limitations

Resolution in a radar system is dependent on factors such as the antenna beamwidth, the transmitted polarization, optimum processing of the received signal, and the waveform selection. This paper considers only the dependency of waveform selection and processing of the received signal on resolution. If the reader desires a more generalized approach to the resolution problem, he is referred to the four-dimensional ambiguity function developed by Urkowitz, Hauer, and Koval to extend

the theory to simultaneous resolution in range, Doppler shift, azimuth, and elevation where the effects of the antenna are included (14).

Resolution and accuracy are two important terms, frequently used in radar parameter estimation, which complement each other but which have distinct differences. Resolution is the ability of a radar to separate two or more targets in a multiple target environment. Accuracy is defined as the closeness of the estimation of a single target's parameters. The plotted ambiguity function gives a good picture of both the accuracy and resolution capabilities of a waveform. In addition, the ambiguity function shows the "proximal" and "distal" ambiguities inherent in each waveform. An ambiguity refers to a difficulty in assignment of a unique position and speed to a target because the matched filter envelope function has appreciable magnitude at more than one point in the ambiguity plane. "Proximal" ambiguities result from a spreading of the central response peak about $\tau = \phi = 0$. "Distal" ambiguities occur at values of $\tau$ and $\phi$ where the ambiguity function has a relatively large amplitude but which are removed from the central response peak. "Distal" ambiguities occur when a periodic waveform is transmitted or when an ambiguity function has a sharply confined central response peak and considerable energy concentrated in its sidelobes.

An estimation of the parameters of a target with a radar operating in a noise environment is, of course, subject to error. Helstrom has shown that the variance in the estimation of the time delay of a received signal when the Doppler shift is known is given by

$$\delta T_r = \frac{1}{B_o\sqrt{2E/N_o}}, \tag{7}$$

and the variance in the estimation of Doppler frequency with a known time delay is

$$\delta\phi = \frac{1}{t_o\sqrt{2E/N_o}} \tag{8}$$

where the signal-to-noise ratio has been assumed to be large in the derivation (15). At first it may appear that increasing both the "effective time duration" and the "effective bandwidth" of the transmitted signal will decrease the variance in the above without limit. Actually such a scheme will decrease the width of the central response peak along both the time delay and Doppler axes. Unfortunately, the ambiguity function increases in length along the major diameter of Helstrom's ellipse as shown in Figure 1. The result is an ellipse with a much smaller minor than major diameter.

The variance along each axis is shown by Helstrom's ellipse when

$$2E/N_o = 1. \tag{9}$$

Should a situation arise such that $2E/N_o$ is known not to equal one, a modification can be made by appropriately raising or lowering the level plane which cuts the ambiguity function so that $\delta\phi$ and $\delta\tau$ still represent the width of the central response peak along the Doppler axis and delay axis, respectively. For comparison of measurement errors inherent

in different waveforms, the quantity $2E/N_o$ is set equal to one.

The radial velocity of an illuminated target is derived from the Doppler shift by the formula

$$V_r = \frac{\lambda\phi}{2} \tag{10}$$

where $V_r$ is the target's radial velocity and $\lambda$ is the transmitted wavelength. The transmitted signal's wavelength can be used to scale the Doppler axis because, for a fixed target velocity, a large wavelength will exhibit a smaller Doppler shift than a smaller wavelength. Hence smaller wavelengths have superior Doppler resolution due to the larger Doppler shifts produced by the moving targets.

The radial range of the target is estimated from the time delay by the formula

$$R = c\Delta t/2 \tag{11}$$

where c is the velocity of light and $\Delta t$ is the time interval between transmitting and receiving the signal.

From Equation (7), increasing the "effective bandwidth" of the transmitted waveform will decrease the error in time delay estimation. A waveform which has a large "effective bandwidth" is a pulse with a short time duration. The ambiguity function for a pulse modulation is

$$|\psi(\tau,\phi)|^2 = \left(1 - \frac{|\tau|}{T}\right) \left\{\frac{\sin\pi\phi T\left(1 - \frac{|\tau|}{T}\right)}{\pi\phi T\left(1 - \frac{|\tau|}{T}\right)}\right\}^2 \quad |\tau| < T \qquad (12)$$

$$= 0 \qquad |\tau| > T$$

where T is the time duration of the pulse. The central response peak is shown shaded in Figure 2. Most of the ambiguity is confined to the Doppler axis and the estimation of time delay can be made very accurately.

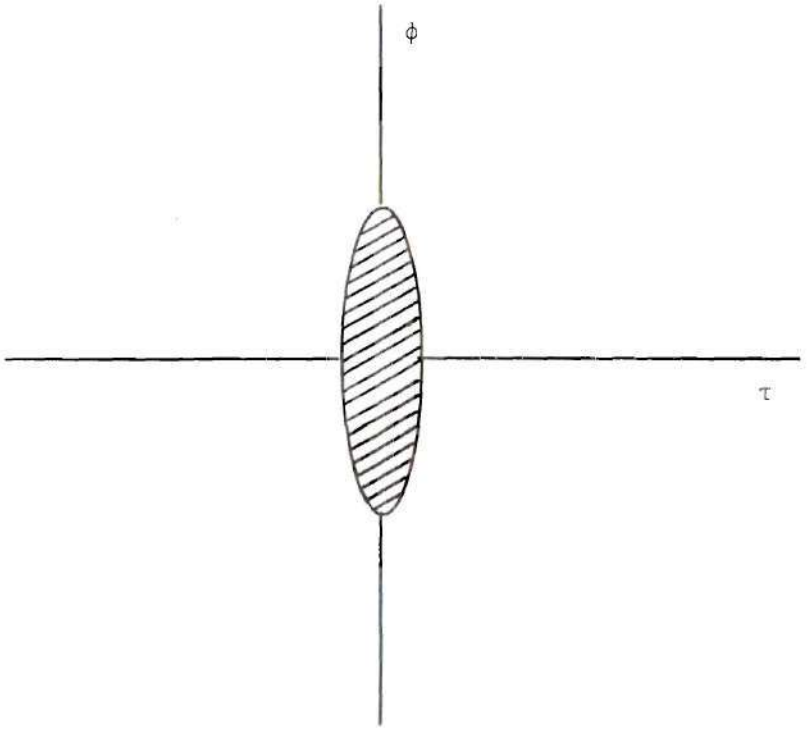


Figure 2. Ambiguity Distribution for a Short Transmitted Pulse

Alternately, from Equation (8), increasing the "effective time duration" of the transmitted waveform will decrease the error in Doppler estimation. If the time duration of the above pulse is increased, the ambiguity is confined mostly to the time delay axis and estimation of Doppler frequency is possible to a high accuracy (Figure 3).

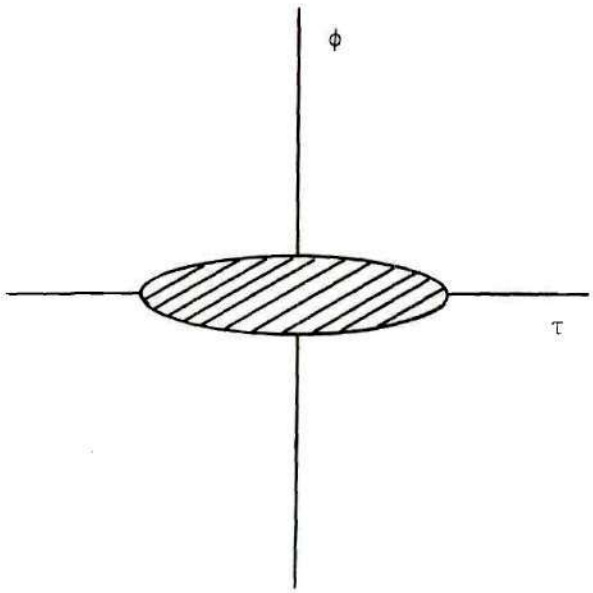


Figure 3. Ambiguity Distribution for a Long Transmitted Pulse

From these examples it appears that increasing the measurement accuracy of one parameter causes a deterioration in the accuracy of measurement of the other parameter. In fact, a formal statement of this heuristic observation takes the form of the uncertainty relation of Gabor (10) which states

$$\beta_o t_o > \pi. \tag{13}$$

There is no upper bound on the time-bandwidth product, only a lower bound. From Inequality (13) it appears that measurement precision for both time delay and Doppler shift will increase if the bandwidth and time duration of the signal increase together. However, a little more care must be taken before a conclusion is reached. Helstrom (16) has shown that a stricter bound for Inequality (13) is

$$\beta_o^2 t_o^2 - \alpha^2 > \pi^2. \tag{14}$$

Helstrom has also calculated the measurement precision when both time delay and Doppler shift must be estimated together (17). The precision of the time delay estimate is

$$\delta\tau = \left(\frac{1}{\beta_o\sqrt{2E/N_o}}\right)\left(\frac{1}{\sqrt{1 - \alpha^2/\beta_o^2 t_o^2}}\right) \tag{15}$$

and the precision of the Doppler shift estimate is

$$\delta\phi = \left(\frac{1}{t_o\sqrt{2E/N_o}}\right)\left(\frac{1}{\sqrt{1 - \alpha^2/\beta_o^2 t_o^2}}\right). \tag{16}$$

Equations (15) and (16) indicate that $\alpha$ should be kept small as the time-bandwidth product is increased for a high resolution.

Unfortunately, most practical methods for increasing the time-bandwidth product, with the exception of a pulse train, cause $\alpha$ to be large. Increases in the time-bandwidth product must be weighed against the detrimental effects of a large effective phase, $\alpha$.

## Resolution in a Multiple Target Environment

In a multiple target environment a radar must be capable of separating targets if a unique position and velocity are to be assigned to each. As the reader may expect, there are fundamental restrictions on the target densities which can be accommodated by a particular radar waveform (18).

High resolution in a dense target environment can be accomplished in two ways, depending on the characteristics of the target environment. First, if the target environment is extended (i.e., a large range of velocities and time delays is expected), a waveform whose ambiguity function has a sharply confined central response peak and a uniform pedestal to distribute the ambiguity volume can be used. Secondly, if the environment is confined, an ambiguity function with a confined central response peak can be used with a clear area extending over the target environment and the remaining ambiguity volume distributed outside the clear area. The limitations in the applicability of these two types of waveforms will now be considered.

### Resolution Limitations in an Extended Target Environment

A waveform useful for the extended target environment must estimate the position and velocity of each target with a high accuracy and must also be free from "distal" ambiguities. A high accuracy requires that the central response peak of the ambiguity function be sharply confined in both the Doppler and time delay dimensions. Freedom from "distal" ambiguities occurs when the ambiguity function is relatively low over all of the ambiguity plane except at the region of the central peak.

An ambiguity function which approximates the above characteristics is the idealized "thumbtack" ambiguity function. This ambiguity function has a sharp peak which is confined in both the time delay and Doppler domains. From Helstrom's ellipse, the extent of the central response peak on the delay axis is $1/\beta_o$, and the extent along the Doppler axis is $1/t_o$. If $\beta_o t_o >> 1$, a necessity for high resolution, the volume under the central response peak is much less than one, since the maximum height of the ambiguity function (Property III) is one. Barring any information about the probable distribution of targets, the best choice for the remaining area would be a low uniform pedestal. If the volume under the central peak of the ambiguity function is negligible, the pedestal must have a height of $1/\beta_o t_o$ to satisfy the unitary volume property (Property V). The "thumbtack" function, Figure 4, is an idealized function which has the above characteristics.

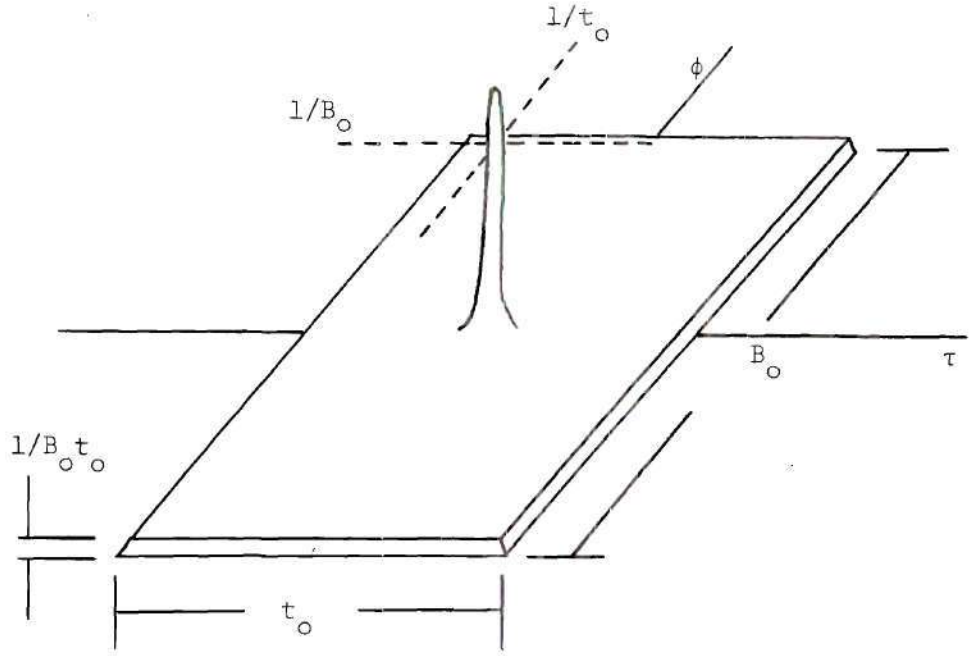


Figure 4. Thumbtack Function

The "thumbtack" function is not realizable, since its uniform pedestal does not satisfy Property VII (self-transform property). Some waveforms, however, have a corresponding ambiguity function with a very confined central response peak and distribute their volume over a relatively low pedestal (7). These ambiguity functions approximate the ideal "thumbtack" function.

The reader may expect, looking at Figure 4, that there is some limit to the number of targets which can be resolved due to the pedestal associated with the "thumbtack" ambiguity function. In fact, there are fundamental limitations to the number of targets which can be resolved.

## Resolution Limitations of the "Thumbtack" Function

The performance of the "thumbtack" ambiguity function will be considered in a uniformly dense target environment. In such an environment each target is assumed to have the same average cross section, and each resolution cell of the ambiguity function contains one and only one target.

The central response peak of the "thumbtack" function has an area of $1/\beta_o t_o$, hence this is the size of a resolution cell. A target having a Doppler shift and time delay anywhere within the area of $1/\beta_o t_o$ around the Doppler delay origin will be assumed to lie at $\tau = \phi = 0$. The number of resolution cells for an effective bandwidth $\beta_o$ and time duration $t_o$ is

$$\text{(number of cells)(area of each)} = \text{total area}$$

$$N(1/\beta_o t_o) = \beta_o t_o \qquad N = (\beta_o t_o)^2. \tag{17}$$

If a signal appears at $\tau = \phi = 0$, the "thumbtack" ambiguity function weights the signal with the constant one. The signal level will be said to be $S = 1$, if a target is at $\tau = \phi = 0$. Since the target environment is assumed to be uniformly dense, each one of the other resolution cells also contains a target with the same average cross section as the target at $\tau = \phi = 0$. The ambiguity function "weights" each of these resolution cells by the magnitude of the ambiguity function at the point $1/\beta_o t_o$. Since there are $N(\beta_o t_o)^2$ of these cells, the total contribution, which is clutter, is

$$C = N(1/\beta_o t_o) = \beta_o t_o. \tag{18}$$

The signal-to-clutter ratio is

$$S/C = 1/\beta_o t_o. \tag{19}$$

For large $\beta_o t_o$ products, the signal-to-clutter ratio becomes small, and it is difficult to estimate the presence of a target at $\tau = \phi = 0$. For a signal-to-clutter ratio of one, $S/C = 1$, the target density is one target per $\beta_o t_o$ cells. Since there are $N = (\beta_o t_o)^2$ cells, the total number of targets is

$$\text{(number of cells)(targets/cell)} = \text{(total number of targets)}$$

$$\text{total number of targets} = \beta_o t_o. \tag{20}$$

These targets can be placed to form another uniformly dense target environment with a resolution cell size of unity. Therefore, for a unity signal-to-clutter ratio the minimum resolution cell is unity in a uniformly dense target environment. Or, if the target density is greater than one target per unit area in the ambiguity plane, the "thumbtack" ambiguity function cannot be used to resolve these targets.

Resolution Limitations in a Confined Target Environment

A confined target environment is one in which the velocities and time delays expected from the received waveform cover a defined range and are not large in extent. Since the uniform pedestal on the "thumbtack" function causes an erroneous estimation of a target's parameters in a dense target environment, a technique for improvement in resolution for the confined target environment is the elimination of the uniform pedestal over the area in the ambiguity plane where targets are expected. It is known that the pedestal cannot be removed over the entire remaining portion of the ambiguity plane because of the volume constraint property (Property V). There must, therefore, be some limit to the clear area which can be located around the central response peak. We will now attempt to find the maximum permissible size of the clear area.

Suppose some waveform exists such that there is no ambiguity along the delay axis for an interval T. Then according to Property IX (Rihaczek volume constraint property), the function along the Doppler axis, which is the Fourier transform of the function on the delay axis, will be relatively free from volume for an interval 1/T.

This result follows from Fourier transform theory and it is not meant to imply that all the volume is removed in the interval. It merely states that the major portion of the volume is removed. The clear area around the central response peak is thus T(1/T) or one.

A waveform whose envelope function is separated in time, such as a pulse train, can be used to remove volume from the central response peak. The ambiguity function for a uniform pulse train is

$$|\psi(\tau,\phi)|^2 = \frac{1}{N^2} \sum_{m=-(N-1)}^{N-1} |\psi_p(\tau-mT,\phi)|^2 \frac{\sin^2\pi\phi(N-|m|)T}{\sin^2\pi\phi T} \qquad (21)$$

where

$$\psi_p(\tau-mT,\phi) = \int_{-\infty}^{\infty} a(t)a^*[t+(\tau-mT)]a^{-j2\pi\phi t}dt, \qquad (22)$$

T is the period, and N is the number of pulses in the pulse train. The ambiguity function has "distal" ambiguities along the Doppler axis every 1/T hertz and along the delay axis every T seconds. The clear area surrounding the central response peak is (2T)(2/T) or 4. However, the target space which can be resolved without interference is half as wide in each domain as the clear area. Therefore, the total unambiguous clear area is one.

Both of the clear areas above have consisted of rectangles and we may desire a bound on a more generally shaped clear area. In addition to proving the maximum rectangular clear area is one, Price and Hofstetter (19) have found the maximum unambiguous elliptically shaped

clear area to be .92. Generally it appears that an unambiguous area of approximately one is the maximum which an ambiguity function can have.

We have seen above that there are fundamental limitations to both the target densities which can be resolved for a particular waveform and the maximum clear area surrounding the origin. In the case of a uniform extended target environment the minimum cell resolution size was found to be unity. For the confined target environment, the maximum clear area surrounding the ambiguity origin is about one. The possibility exists for a high resolution in the confined target environment if it can be scaled to "fit" the unit clear area constraint. As we will see in Chapter IV, the wavelength chosen for transmission can be used to spread or confine the probable target Doppler shifts. This independent wavelength adjustment can sometimes be used to scale the expected Doppler shifts to fit in the clear region.

# CHAPTER IV

## APPLICATIONS OF THE AMBIGUITY FUNCTION

The ambiguity function's utility is in the selection of optimum waveforms for transmission. This function not only gives a clear indication of ambiguous, undesired responses for a given waveform, but it also shows the resolution capability of the waveform and the precision of the Doppler and time delay estimates from the waveform.

The selection of a waveform for transmission cannot be effectively accomplished until some characteristics of the target environment are known. In general, if we know some properties of a particular target environment, the transmitted waveform can be selected to greatly enhance target detection. Alternately, if there is no information about the probable number of targets, the distribution of the targets in range and velocity, or the contribution to the radar echo due to clutter, then it is impossible to select an optimum waveform.

As mentioned in Chapter III, the function of a modern radar is not only to detect the presence of a target but also to determine how many targets contribute to the combined radar return and to estimate the radial velocity and radial range of each of these targets with the highest possible accuracy. Siebert has shown that detection of a target is dependent only on the energy content in the transmitted waveform (20). Distinguishing the number of targets in a multiple target environment places demands on the resolution capability of a waveform.

Estimating the velocity and range with a low error necessitates a waveform with high accuracy. In addition, ambiguities must be eliminated if a target is to be resolved from a collection of scatterers or if an accurate range and velocity are to be assigned to a target. Waveform design must encompass all of these requirements and deal with each satisfactorily to have a useful radar system. In other words:

(1) We must transmit enough energy for the reflected wave to be detected at the receiver.

(2) The waveform must have high enough resolution to separate the targets into individual returns.

(3) The waveform must have sufficient accuracy to estimate the velocity and range of an individual scatterer with a low error.

(4) Ambiguous responses of the matched filter, which are far from the central response peak, must either be eliminated or positioned such that a target never appears on an ambiguous peak.

## Some Synthesis Techniques for Clutter Rejection

The most straightforward approach to optimum waveform selection would be to investigate the target environment, select regions in the ambiguity plane where a response is desired from the matched filter output, and then synthesize a waveform which has the desired energy, resolution, accuracy, and ambiguity distribution. Unfortunately, the problem cannot usually be approached directly because an effective general synthesis technique for ambiguity functions does not exist.

Although no general synthesis technique exists for ambiguity functions, two special techniques have been developed and are useful in

cases where the clutter distribution is known. The first of these techniques is used to find an optimum set of phase and amplitude weightings for coherent pulse train signals. W. D. Rummler has developed an iterative technique which uses a computer to determine optimum weightings (21). The criterion of performance of the codes is taken to be the signal-to-interference ratio where the interference is due to noise and returns from clutter. The signal-to-interference ratio is the ratio of the square of the peak signal voltage to the mean square noise voltage plus the mean square voltage due to clutter. Optimum receiver weightings are used for the transmitted signal to generate a new set of optimum receiver weights and the process continues until the procedure converges. Note that the convergence is not necessarily a matched filter result, which indicates different weightings will be used for the transmitted waveform than those which are used for the received waveform. In general, if the clutter is symmetrical about the origin, the procedure will converge so that the receiver filter is matched to the transmitted waveform. The most serious defect of this optimization procedure is that the result of the calculation depends on the initial choice for the weighting. Rummler argues that the dependence of the signal-to-interference ratio on the initially chosen weightings is not strong. Therefore, a useful result is obtained regardless of the initial choice for the weightings.

Another synthesis technique has been developed by William Blau for three classes of time-frequency codes:

(1) Uniform amplitude, uniform pulsewidth matched codes.

(2) Uniform amplitude, nonuniform pulsewidth matched codes.

(3) Uniform amplitude, uniform pulsewidth with receiver mismatch (22). This technique shapes the central response peak to specifications. A model is first used for the desired ambiguity function and an approximation to the desired function is generated using Monte Carlo techniques for the selection of a set of time delays and relative phases for the individual pulses. This process is continued until the generated central response region conforms to the desired one.

Both of these synthesis techniques described above are useful for generating pulse train waveforms with desired clutter rejection characteristics. However, both of the techniques have weaknesses. The first technique leads to a non-unique solution and the synthesis technique of Blau shapes only the central response peak of the ambiguity function.

## Differentiation of Clutter from Desired Targets

Occasionally, either the position or velocity of a body of clutter is known and differs from that of the expected targets. In this case the targets may be differentiated from background clutter by an appropriate waveform.

For a body of clutter in a known position, discrimination between targets and clutter is achieved by ignoring the radar return during the time period when the return is due to clutter.

Discrimination between targets and clutter on a velocity basis is also possible. Manuel Ares has described a technique which can generate a burst waveform which gives optimum target detection in

range-extended clutter (23). The technique minimizes the clutter-to-signal ratio with a minimum signal-to-noise degradation. The inter-pulse spacing is assumed fixed and the phase and amplitude of each pulse are adjusted so that the ambiguity function does not have a large value for Doppler shifts corresponding to the clutter. Ares has obtained solutions for bursts of length three to eight pulses. Although mismatched filters were considered, the optimum results were obtained for the matched filter case. A similar technique has been used by C. P. Rasmussen to give effective waveforms for clutter discrimination (24).

Rihaczek and Mitchell have considered clutter which has a more complex orientation in position and Doppler (25). Consider the extended clutter in Figure 5. The approach used by the authors is to confine the ambiguity function in a strip which includes as little of the clutter space as possible. Although strict confining of the ambiguity function is found to be impossible, a rectangular pulse with a quadratic phase modulation can be used to approximate the desired ambiguity surface.

Using the ambiguity function for improving performance of radar in clutter is impossible unless the distribution of the clutter is known and the clutter can be differentiated from the desired targets by either Doppler shift or time delay. In a large number of problems clutter is either not present or nothing is known about its characteristics. For these problems, an ambiguity function is desired which has a confined central response peak for high resolution and a low sidelobe level for

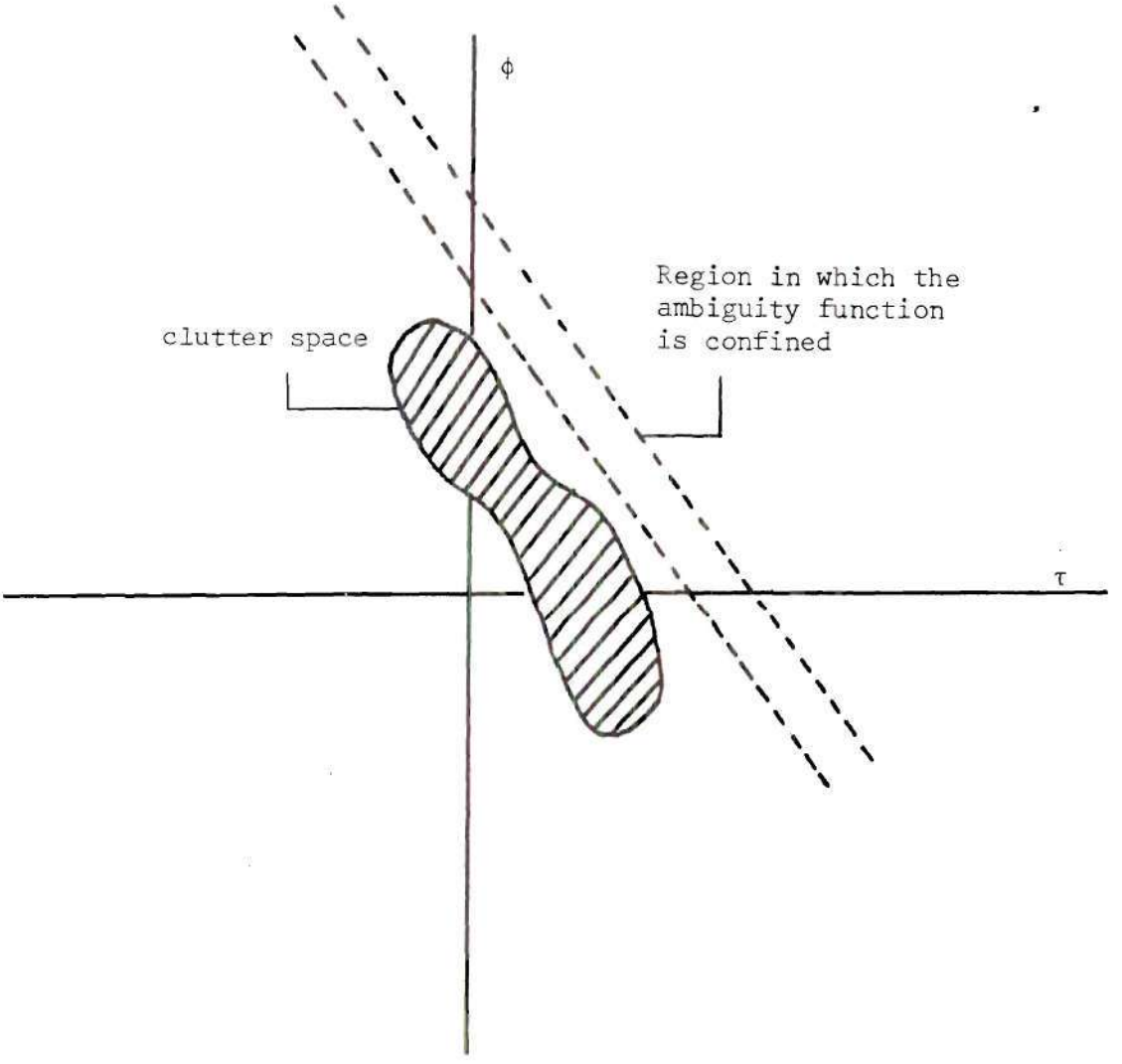


Figure 5. A Complex Clutter Space

clutter rejection. Several waveforms which are suitable for the unknown clutter target environment will now be considered both for the light target and dense target cases.

## Light Target Environment

A light target environment is defined as one in which only a few targets appear and the return due to clutter is not significant. An

ideal ambiguity function for the light target case would have the characteristics of the "thumbtack" function. The sharp peak of the "thumbtack" function would eliminate most of the inaccuracy associated with the determination of range and velocity. The low pedestal, which must accompany the sharp peak due to Property V, does no harm because only a few targets are assumed present. A threshold decision can be made at the filter output to effectively eliminate ambiguous responses from undesired targets and give an estimate of each target's location and speed, provided the targets are separated sufficiently to be resolved. No waveform can have an ambiguity function exactly equivalent to the ideal "thumbtack" function because the pedestal does not satisfy Property VIII.

However, in search of a waveform which approximates the "thumbtack" function by being confined in both the Doppler and time delay domains, J. R. Klauder formulated the rotational invariance property (Property X) (7). Klauder's waveforms, rotationally invariant on the ambiguity plane, are defined by

$$u_n(t) = \frac{(2)^{1/4}}{\sqrt{n!}} e^{-\pi t^2} H_n(2\sqrt{\pi}t) \tag{1}$$

where $H_n(x)$ is the nth order Hermite polynomial given by

$$H_n(x) = (-1)^n e^{x^2/2} \frac{d^n}{dx^n} e^{-x^2/2}. \tag{2}$$

The ambiguity function for these waveforms is

$$|\psi_n(\tau,\phi)|^2 = |e^{-\pi/2(\tau^2+\phi^2)} L_n[\pi(\tau^2+\phi^2)]|^2, \tag{3}$$

where

$$L_n(x) = \sum_{K=0}^{n} \frac{n!(-x)^K}{(n-K)!K!} . \tag{4}$$

The rotational invariance property can be demonstrated by noting that

$$\tau'^2 + \phi'^2 = \tau^2(\cos^2\theta+\sin^2\theta) + \phi^2(\cos^2\theta+\sin^2\theta) = \tau^2 + \phi^2 \tag{5}$$

where $\tau'$ and $\phi'$ represent the orthogonal components of the rotated axis and $\theta$ is the angle of rotation.

Since these waveforms are rotationally invariant, a two-dimensional plot of their respective ambiguity functions is sufficient for a complete understanding of the ambiguity surface. Ambiguity functions have been plotted for $n = 4$ and $n = 10$ (Figure 6). As seen from the figure, these waveforms have relatively low sidelobes and no difficulty arises in locating the target position and speed within the region covered by the central response peak of the waveform. Note that the transmitted waveform can be scaled in time to reduce the width of the central response peak in range and hence increase its precision, but velocity resolution must suffer.

Although this waveform gives some pleasing analytical results, it is too difficult to transmit and the matched filter is too

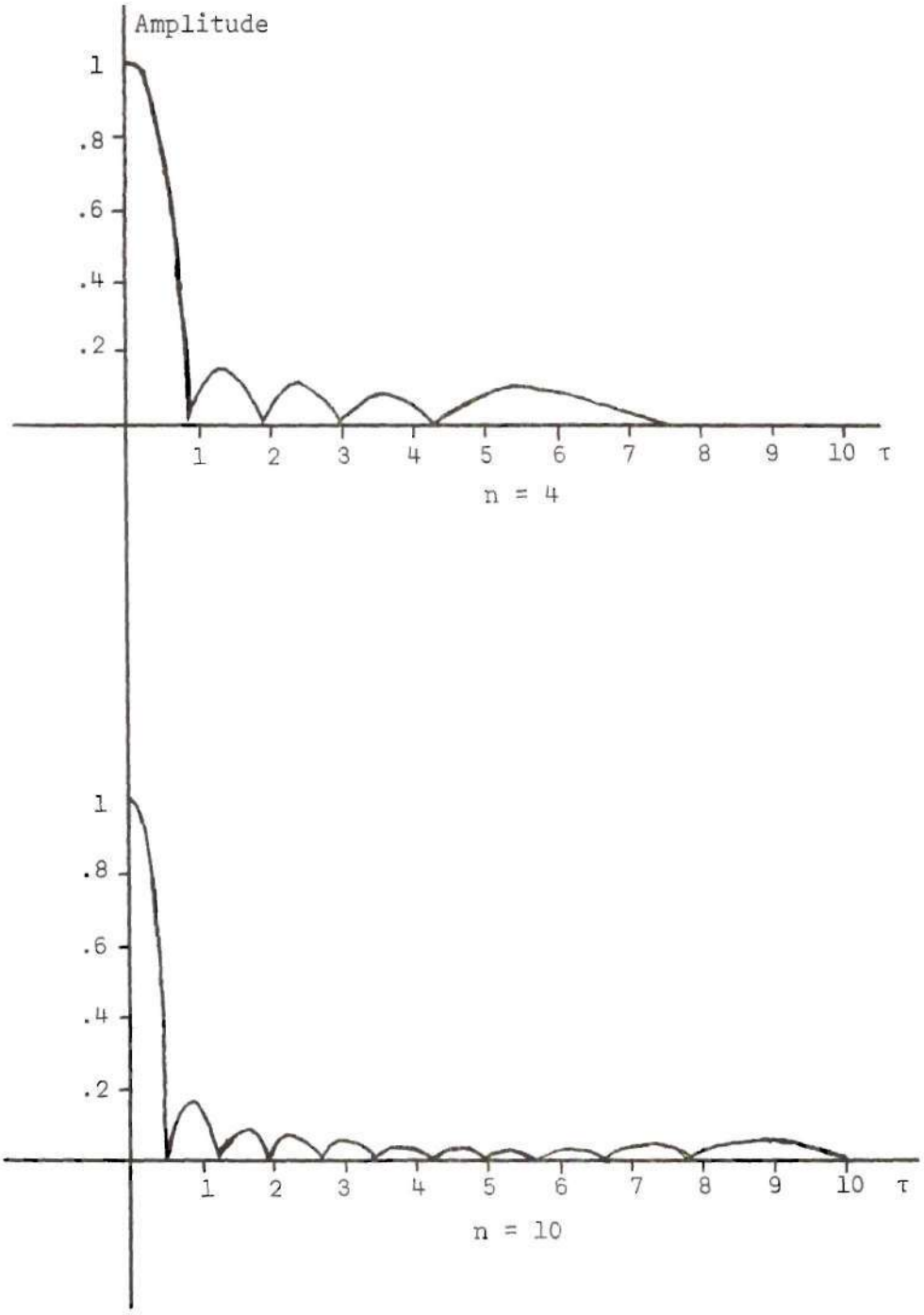


Figure 6. Ambiguity Surfaces for Klauder Waveforms with n = 4 and n = 10

complicated to make the waveform practical in a simple system. But more importantly, the waveform does not have a constant envelope and therefore does not make optimum use of the transmitter's peak power.

## Linear V--FM

A more practical, although still complex, waveform which gives good resolution in both Doppler and time delay is the linear V-FM pulse given by

$$u(t) = u_1(t) + u_2(t) \qquad -T < t < T \tag{6}$$

$$= 0 \quad \text{elsewhere}$$

where

$$u_1(t) = \frac{1}{\sqrt{2T}} e^{-jbt^2} \qquad -T < t < 0 \tag{7}$$

$$= 0 \quad \text{elsewhere}$$

and

$$u_2(t) = \frac{1}{\sqrt{2T}} e^{jbt^2} \qquad 0 < t < T \tag{8}$$

$$= 0 \quad \text{elsewhere.}$$

The central response peak for the ambiguity function is shown in Figure 7. Targets which appear at Doppler frequencies which do not

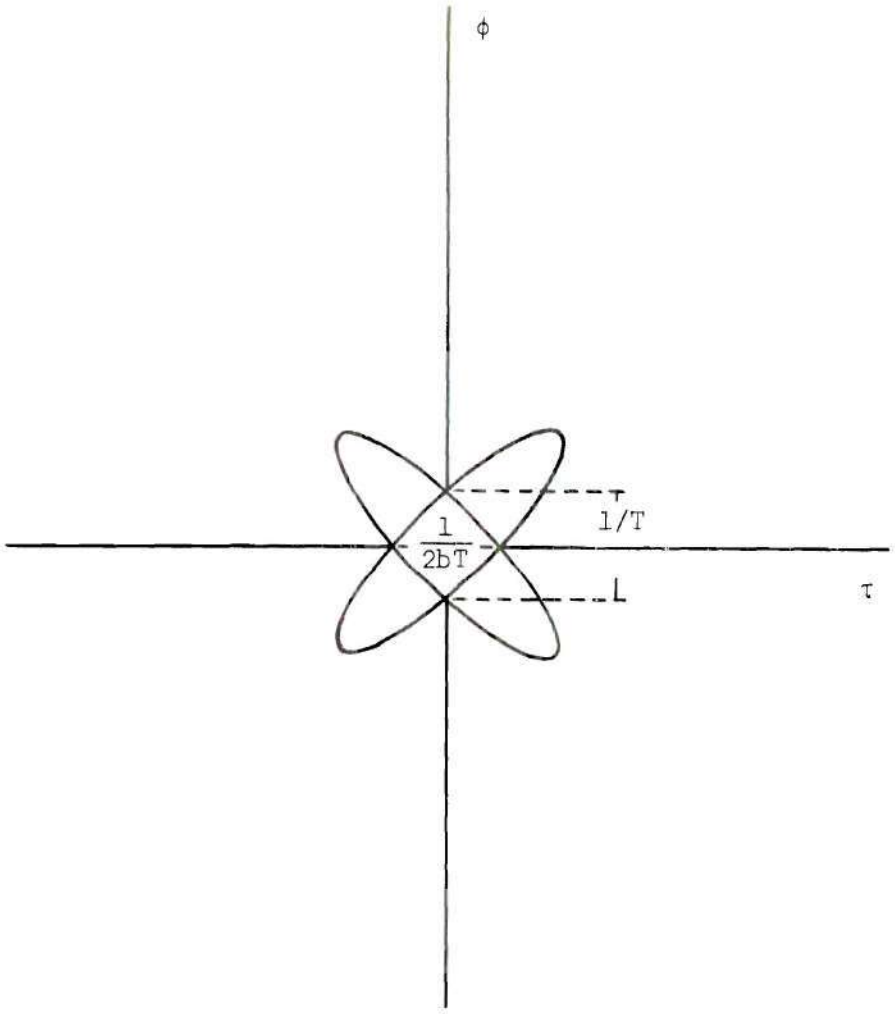


Figure 7. Ambiguity Distribution for the Linear V-FM Waveform

correspond to the center frequency of the matched filter will produce two returns which differ in time delay. For the single target case, the filter matched to the Doppler shift of the target can easily be found because it is the only filter which has one output versus time. In a light target environment a filter matched to a target produces an odd number of returns, whereas filters which are not matched in Doppler

to any target produce an even number of outputs versus time. Theoretically, the linear V-FM waveform offers simultaneous resolution, in both Doppler and time delay, limited only by the dimensions of the central response peak. In actuality, resolution is possible only in a light target environment where targets are not closely spaced in either velocity or position.

## Multiple Target Resolution in Range

As we saw in Property XI (Taylor series), good resolution in range requires a large effective bandwidth. A pulse with a very short time duration, and hence a large bandwidth, can give excellent range resolution but may not contain enough energy for its reflection to be covered from background noise. When detection requirements and peak power limitations force an abandonment of the simple short pulse, other waveforms with both a high energy and a large effective bandwidth must be used.

Since a radar is usually limited in its peak power, the time duration of the waveform must be increased to increase the energy content. At first it may seem that increasing both the bandwidth and time duration of the signal is impossible. However, many waveforms have both long time durations and large bandwidths, and some of these waveforms will now be investigated.

For $\phi = 0$ the ambiguity function is just the squared magnitude of the autocorrelation function of the normalized transmitted waveform. Therefore, it is important to note that range resolution is better with a confined autocorrelation function. Fortunately, numerous high energy

waveforms with good autocorrelation properties and a long time duration exist (26). Here a waveform is considered to have good autocorrelation properties if the width of the ambiguity function along the $\tau$ axis is much less than the transmitted signal's duration. Waveform codes with good autocorrelation properties consist of pulse trains where either the interval between pulses or the pulse phase is coded. These waveforms are particularly suited for resolution in range where the velocity of the target is either known or can be derived in some other manner. Two groups of waveforms presented by Pettit are very useful in radar applications.

Barker Codes

One set of waveforms with good autocorrelation properties is the Barker set where the two Barker symbols are transmitted through the phase of the signal and the two states differ in phase by 180°. The velocity spread of the targets must be small when using the Barker codes because they have large ambiguous responses for Doppler frequencies off center. Barker codes have been found with lengths of 3, 4, 5, 7, 11, and 13 (Figure 8). These codes have the property that the magnitude of their autocorrelation function does not exceed 1/N for $|\tau| > T$ where the autocorrelation function is normalized to unit height, N is the number of pulses in the code, and T is the individual pulse width. In Figure 9 the autocorrelation functions of some Barker codes are shown. The resolution of these codes is $\Delta R = cT/2$ for an individual pulse width T. The actual signal has a duration of NT, but the range resolution of this waveform is dependent only on the individual pulse width.

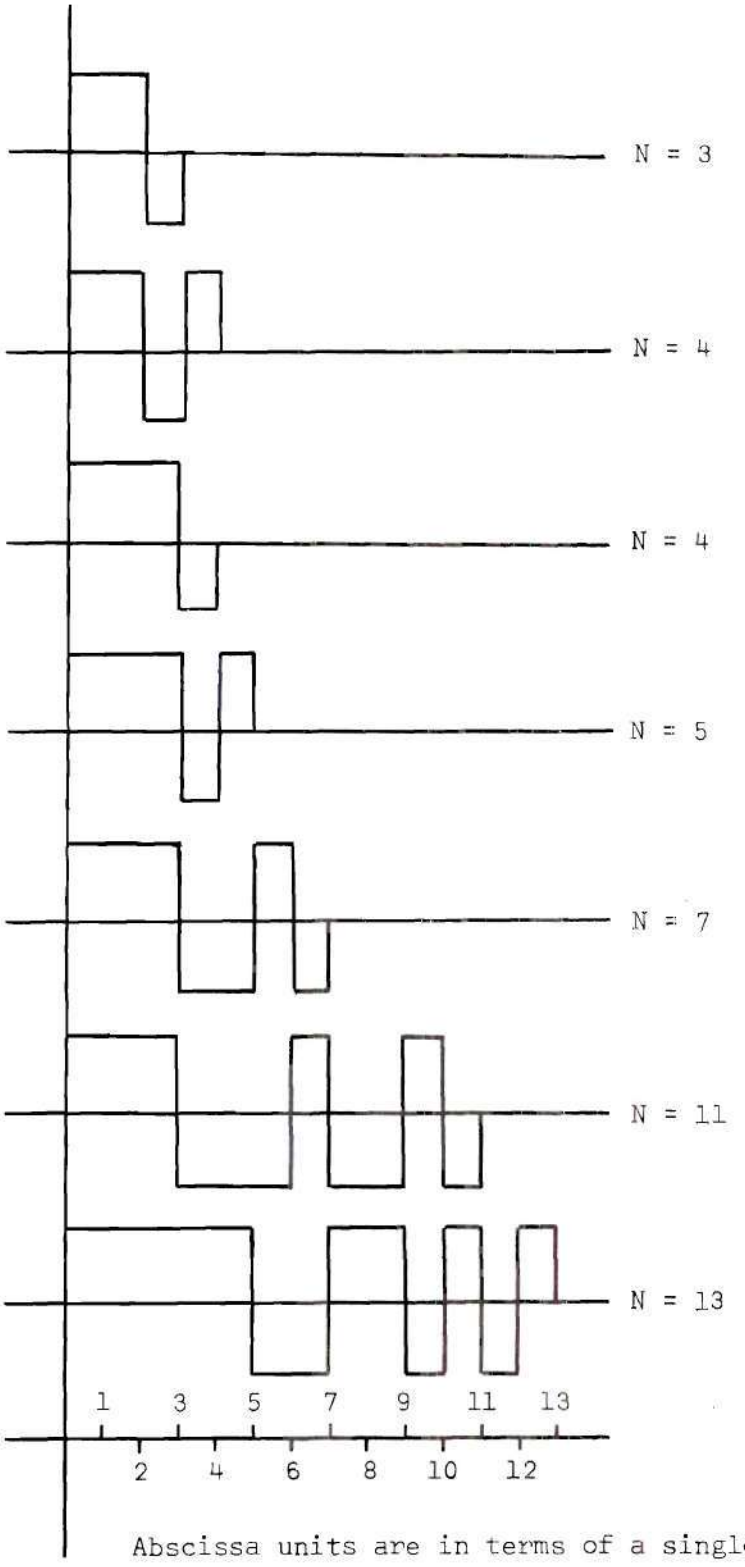


Abscissa units are in terms of a single pulse width.

Figure 8. Waveforms of the Barker Codes

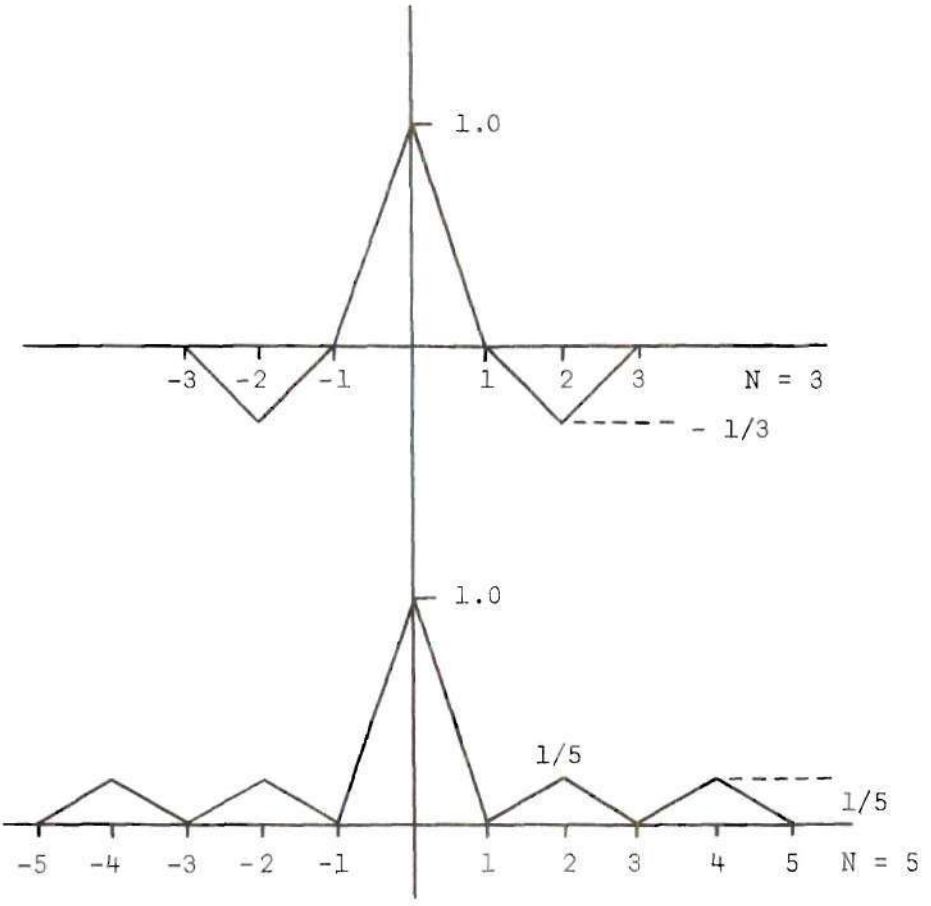


Abscissa units are in terms of the individual pulse width.

Figure 9. The Autocorrelation Function of Barker Codes with Lengths N = 3 and N = 5

Resnick Waveforms

Another class of waveforms with high resolution has been investigated by Resnick (27). These coded waveforms also have the property that their autocorrelation function does not exceed 1/N for $|\tau| > T$ where T is the individual pulse duration and N is the number of pulses in the code. Some codes of this class are plotted in Figure 10.

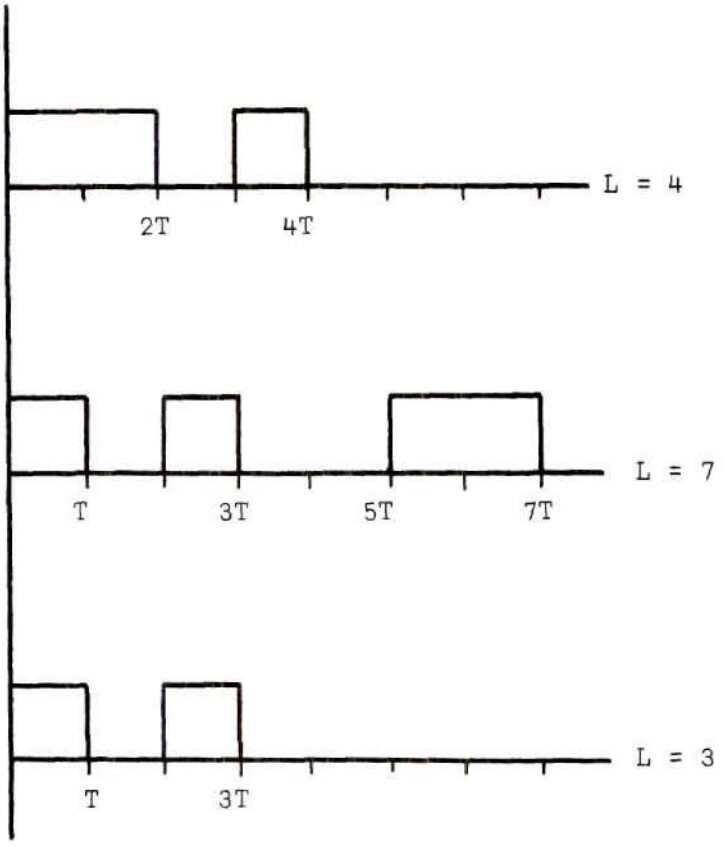


Figure 10. Waveforms of the Resnick Class

These codes are synthesized by noting that the distance between any two pulses, not necessarily adjacent, must be unique. The adjustment of unique distances between the pulses eliminates any large off-Doppler ambiguities. This can be shown from

$$\int_{-\infty}^{\infty} u(t)u^{*}(t+\tau)e^{-j2\pi\phi t}dt, \tag{9}$$

the equation for $\psi(\tau,\phi)$.

Note that for $\phi = 0$, $e^{-j2\pi\phi t}$ is equal to one, therefore the integral reduces to

$$\int_{-\infty}^{\infty} u(t)u(t+\tau)dt \qquad (10)$$

where in the Resnick waveforms u(t) is real. For any values of t and $\tau$ the integrand in Equation (10) is greater than or equal to zero. Now for some other constant value of Doppler shift the integral becomes

$$\int_{-\infty}^{\infty} u(t)u(t+\tau)e^{-j2\pi\phi_o t}\, dt. \qquad (11)$$

If the pulses are the same distance apart, then they are in phase under the integral when the product of the pulse spacing and $\phi_o$ is an integer. The integrand then becomes

$$u(t)u(t+\tau)dt \qquad (12)$$

as before because the phase term is $e^{-j2\pi}$. Since the integrand is again non-negative for all values of $\tau$ and t, the integral is a relative maximum.

Adjustment of the pulses so that their distances are unique assures that the pulses will never all be in phase for some Doppler. This adjustment eliminates any large responses for a Doppler shift not matched to the filter because the phase term, $e^{j2\pi\phi t}$, causes the integrand to be both positive and negative. In fact, variation in the Doppler domain, for a constant $\tau$, never exceeds the value of the

ambiguity function on the $\tau$ axis (Property XII). Therefore, these waveforms, with unique spacing between pulses, produce an ambiguity function which is relatively low over most of the ambiguity plane.

Linear FM Waveform

A final example of a waveform suitable for accurate estimation of target range, when velocity is known, is the linear FM waveform. As shown in Property VI, if $\psi(\tau,\phi)$ corresponds to $u(t)$, then $\psi(\tau,\phi+K\tau/\pi)$ corresponds to $u(t)e^{jKt^2}$. Quadratic phase modulation of the transmitted waveform gives an ambiguity function that has a shifted central response peak when compared with the ambiguity function associated with the envelope $u(t)$. A plan view of the central response peak is shaded in Figure 11.

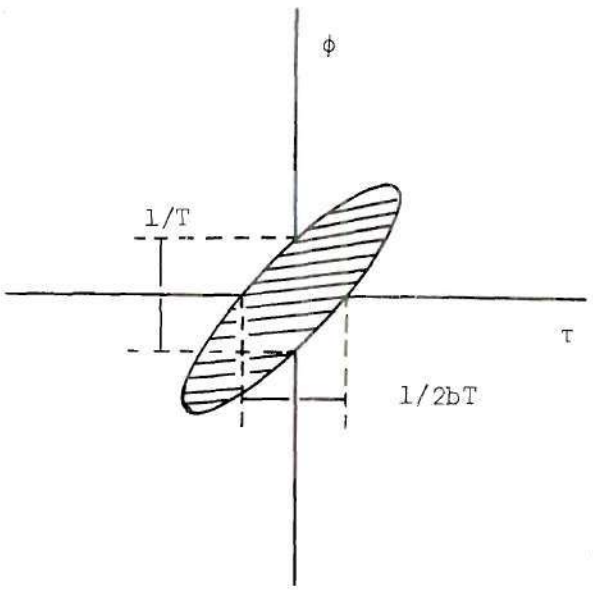


Figure 11. Central Response Peak of the Ambiguity Function of the Linear FM Waveform

The ambiguity function is

$$|\psi(\tau,\phi)|^2 = \left(1 - \frac{|\tau|}{T}\right)^2 \frac{\sin^2([b\tau-\pi\phi][T-|\tau|])}{([b\tau-\pi\phi][T-|\tau|])^2} . \qquad (13)$$

The linear FM waveform is very important in applications because of the ease with which it can be transmitted and also because of the high resolution possible with a long time duration, and hence high energy, waveform.

The linear FM technique is often called pulse compression (28). As can be seen from Figure 11, the width of the central response peak, for a constant $\phi$, is much less than the width of the transmitted pulse. This decrease in width greatly decreases the range resolution cell size.

Looking at the ambiguity diagram, the response of an approaching target, with positive Doppler shift, will lag a stationary target at the same range, and the response of a receding target will emerge before the stationary target at the same range (29). There is, therefore, an error in the estimation of range for moving targets. The time lag, $t_\ell$, is

$$t = - \phi/2b = - V_r/\lambda b. \qquad (14)$$

This corresponds to a range error, $R_e$, of

$$R_e = - c/2(V_r/\lambda b). \qquad (15)$$

The illuminated target will move the distance $R_e$ in $t_e$ seconds where

$$t_e = - c/2\lambda b. \tag{16}$$

This time error is independent of target velocity. If a time equal to $t_e$ is subtracted from the estimated time of the target, the new time corresponds to the true target range regardless of the target's velocity. This constant delay can easily be incorporated into the radar system to give accurate estimation of target range regardless of the Doppler frequency shift.

The precision of the range estimate from the linear FM waveform is dependent on its "effective bandwidth." Skolnik has shown that the square of the "effective bandwidth" is given by

$$\beta_o^2 = \frac{\frac{\pi^2 B^2}{3} - \pi B^2 \frac{\sin \pi BT}{2BT} + \frac{\pi B^2 S(\pi BT)}{(2BT)^{3/2}}}{1 + \frac{C(\pi BT)}{(2BT)^{1/2}}} \tag{17}$$

where

$$S(u) = \int_o^u \sin \frac{\pi}{2} y^2 dy, \tag{18}$$

$$C(u) = \int_o^u \cos \frac{\pi}{2} y^2 dy, \tag{19}$$

$B = 2bT$ is the width of the swept frequency, and T is the time duration of the waveform (30). As $BT \to \infty$, $\beta_o^2 \to \pi B^3/3$, and therefore for large time-bandwidth products the "effective bandwidth" is approximated by

$$\beta_o \approx \pi B/\sqrt{3} \quad . \tag{20}$$

From Helstrom's ellipse, the width of the central response peak on the delay axis is $1/\beta_o$ and is given by $\sqrt{3}/\pi B$ for large time-bandwidth products. Range resolution can therefore be enhanced by increasing the swept bandwidth. Plots of the ambiguity function for $\phi = 0$ are shown in Figure 12 for TB = 25 and TB = 50.

The range sidelobes, evident in the figure, sometimes cause an erroneous estimation of position from a strong target. Various weighting techniques have been investigated to reduce these range sidelobes (31). Both unilateral and bilateral Hamming weighting has been used to reduce these sidelobes without degrading the signal-to-noise ratio significantly. Unilateral weighting is applied only to the receiver filter, while the transmitted waveform is undisturbed. Bilateral weighting adjusts both the transmitted waveform and the receiver filter response.

## Simultaneous Estimation of Velocity and Position in a Multiple Target Environment

When a radar is operated in a dense target environment, a resolution problem exists. If a unique radial position and radial velocity are to be assigned to each target, the radar must be capable of viewing each target separately. An ambiguity function which is unambiguous would confine most of its response in its central response peak and have a minimum sidelobe level. Due to the volume constraint, an ambiguity function confined to only a central response peak must have an extended central response peak and therefore have low precision.

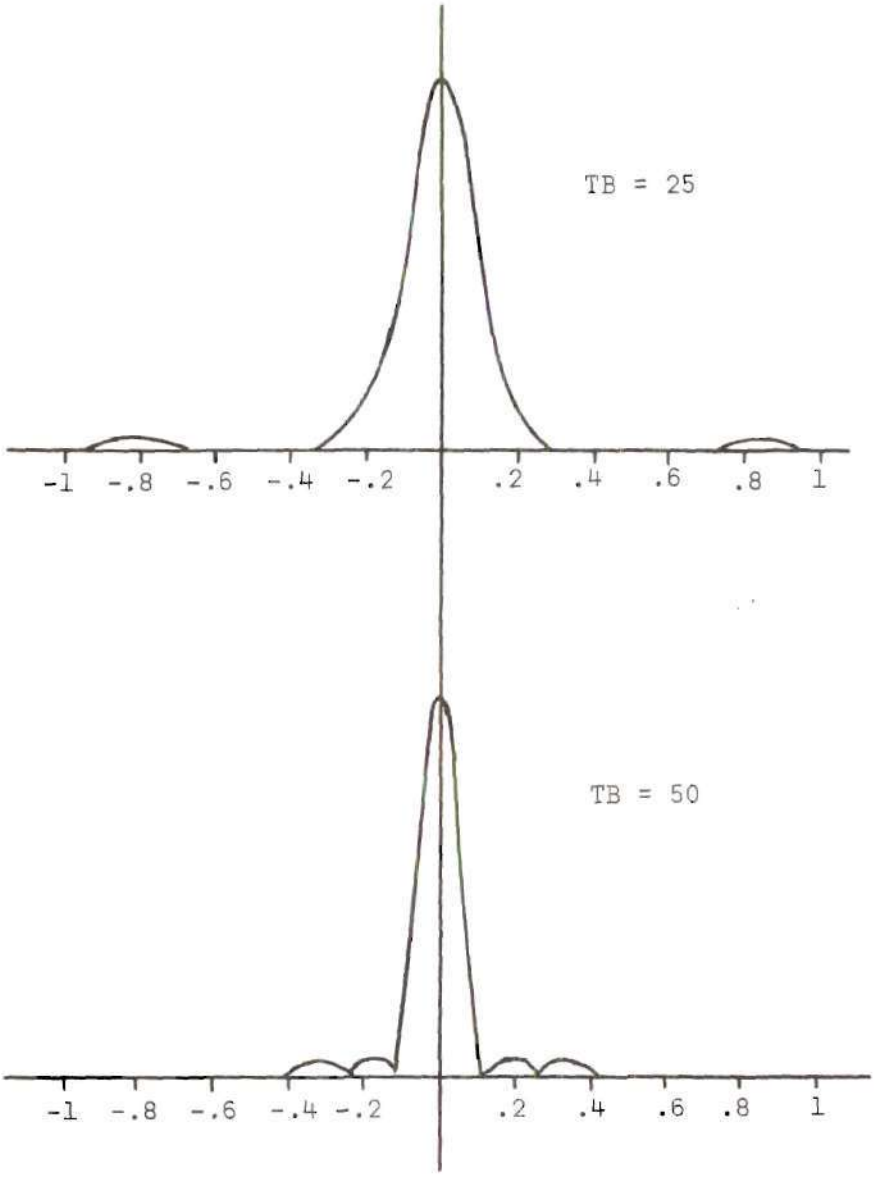


Abscissa units are in terms of the individual pulse width.

Figure 12. The Linear FM Waveform Along the Delay Axis for TB = 25 and TB = 50

Alternately, a waveform may be transmitted with a small central area and with the remaining responses appearing for Doppler shifts or time delays which are not expected.

Pulse trains find the most general use for this case because they are easy to generate and they are capable of high resolution in both Doppler and time delay, although they do possess large ambiguous responses for Doppler and time delays off the filter design center. The design of the waveform must take into account these ambiguities and avoid large off-Doppler center responses for expected target parameters.

A good waveform for the multiple target case is a burst of a coherent train of equally-spaced pulses. The ambiguity function is given by

$$|\psi(\tau,\phi)|^2 = \frac{1}{N^2} \sum_{m=-(N-1)}^{(N-1)} |\psi_p(\tau-mT,\phi)|^2 \frac{\sin^2\pi\phi(N-|m|)T}{\sin^2\pi\phi T} \qquad (21)$$

where

$$|\psi_p(\tau-mT,\phi)|^2 = \left|\int_{-\infty}^{\infty} u(t)u(t-[\tau-mT])e^{j2\pi\phi t}dt\right|^2. \quad (32) \quad (22)$$

The ambiguity pattern for this waveform is shown in Figure 13. The first Doppler ambiguity occurs at $\phi = 1/T_r$ and the first time delay ambiguity occurs for $\tau = \pm T_r$. There is a clear area of magnitude four where no large distal ambiguities exist. Therefore, the maximum unambiguous clear area is one. This means that if the product of the expected maximum Doppler shift and maximum time delay is one, the pulse

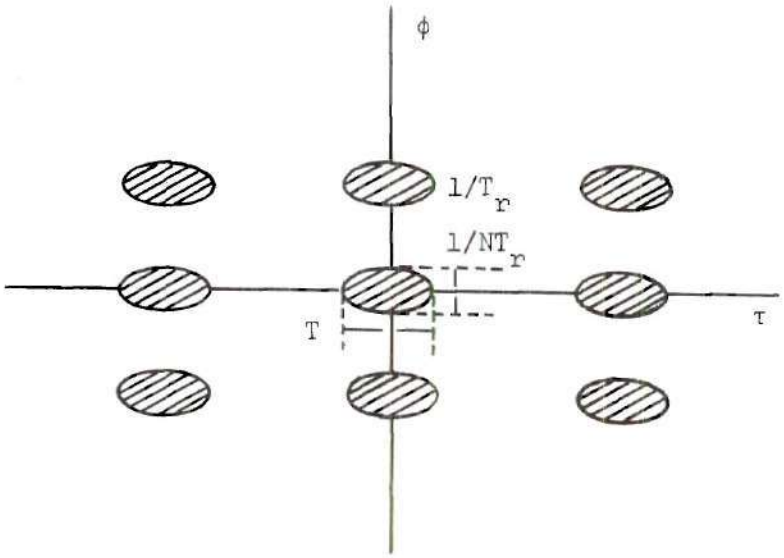


The individual pulse width is T and $T_r$ is the distance between pulses.

Figure 13. Central Portion of the Ambiguity Surface of the Uniform Pulse Train

train burst can be designed to avoid distal ambiguities. Translated into velocity and range the bound on the product becomes

$$\left(\frac{4|V_r|}{\lambda}\right)\left(\frac{2R}{c}\right) \leq 1 \tag{23}$$

or

$$|V_r|R \leq c\lambda/8. \tag{24}$$

If the product of the maximum expected radial range and radial velocity is greater than $c\lambda/8$, the equally spaced pulse train cannot be designed to avoid distal ambiguities. An increase in the transmitted wavelength

will increase the size of the target area which can be accommodated, but the increase in wavelength also causes the Doppler resolution of the radar to suffer.

The precision of the Doppler estimation depends on the number of pulses which are in the burst waveform and the pulse spacing. The central response peak of the ambiguity function has an extent of approximately $1/NT_r$ in the Doppler domain where N is the number of pulses in the waveform and $T_r$ is the pulse separation. The width of an individual pulse can be chosen to fix the range resolution cell to the desired size.

An illustration of the adjustment of pulse width, pulse duration, and pulse spacing will now be given. Consider the possibility of achieving these system requirements:

Resolution in Range.....100 meters

Resolution in Velocity.....30 m/s

Maximum Range.....200,000 meters

Maximum Velocity.....400 m/s.

We may make the hypothesis that this radar will be used in a search mode and its probable targets are helicopters and airplanes. The maximum range requirement may come about because of time needed to prepare for an attack, and the velocity resolution capability can be used to separate slow and fast moving aircraft. The range resolution requirement arises from a desire to separate the targets and estimate their number from a distance.

First the maximum velocity range must be checked with the time duration and the bandwidth of the transmitted waveform to see if the

ambiguity function is a valid model for the given parameters. The time duration and bandwidth of the waveform follow directly from the resolution desired in velocity and range where

$$\text{Time duration} = T_r = \frac{\lambda}{(2)\Delta V_r} \tag{25}$$

and

$$\text{Bandwidth} = \{\frac{1}{B}\frac{c}{2} = \Delta R\} \tag{26}$$

$$= B = c/2\Delta R.$$

Using the inequality from Chapter III we find

$$V_{MAX} << c/(2)(T_t)(B), \tag{27}$$

$$V_{MAX} << c/(2)\left(\frac{\lambda}{2\Delta V_r}\right)\left(\frac{c}{2\Delta R}\right), \tag{28}$$

and

$$V_{MAX} << \frac{(2)(\Delta V_r \text{ m/s})\Delta R(\text{meters})}{\lambda(\text{meters})}. \tag{29}$$

For this example $\Delta V_r$ = 30 m/s, $\Delta R$ = 100 meters, and $V_{MAX}$ = 400 m/s. Therefore, $\lambda$ << 15 meters for these parameters. As long as our selected wavelength is much less than 15 meters, the time compression of the waveform can be neglected and the ambiguity function assumptions are valid.

Let us attempt to design the pulse burst so that no Doppler ambiguities are present. From an examination of Figure 13, the individual pulse width is fixed by the desired resolution in range. The pulse width is therefore

$$cT/2 = \Delta R = 100$$
$$T = 2 \times 10^{-6} \text{ seconds.} \tag{30}$$

The maximum range which we desire to explore will fix the minimum spacing between pulses. This spacing is

$$T_r = \frac{(2)R_{MAX}}{c} = \frac{4}{3} \times 10^{-3} \text{ seconds.} \tag{31}$$

Our desired velocity resolution will determine the number of pulses which are needed in the burst waveform. This is seen by noting from Figure 13 that the spreading of the central response peak is given by

$$\Delta\phi = 1/NT_r. \tag{32}$$

Now solving for the number of pulses we have

$$\frac{(2)(\Delta V_r)}{\lambda} = \frac{1}{NT_r}, \tag{33}$$

and

$$N = 125\,\lambda \tag{34}$$

where $\lambda$ is expressed in meters. It can now be seen that an adjustment which depends on the transmitted wavelength is possible for the desired velocity resolution. Long wavelengths require a long pulse train or a large time duration, whereas short wavelengths have a greater resolution capability. Before a wavelength selection is made, however, one additional constraint must be satisfied. We desire that no Doppler ambiguities appear for a spread of velocities of ±400 meters per second. The distance to the first Doppler ambiguity is $\phi = 1/T_r$. Expressed in meters per second, the magnitude of the maximum is

$$|V_{MAX}| = \frac{\lambda}{4T_r} = \frac{375\lambda}{2} . \tag{35}$$

Our desired wavelength, therefore, must be 2.14 meters or greater to avoid Doppler ambiguities. Looking back to Equation (34) for the length of the burst waveform, we find that a burst of length $N = 268$ must be transmitted to achieve the design parameters. This waveform would have a duration of about $358 \times 10^{-3}$ seconds. Implicit in our ambiguity function model is the assumption that target acceleration can be neglected over the duration of the transmitted signal. For a waveform of length 358 ms, this assumption is not a good one.

One solution to the resolution of Doppler ambiguities has been suggested by H. H. Woerrlein (33). Suppose a staggered pulse train is transmitted having the form shown in Figure 14. The receiver, which

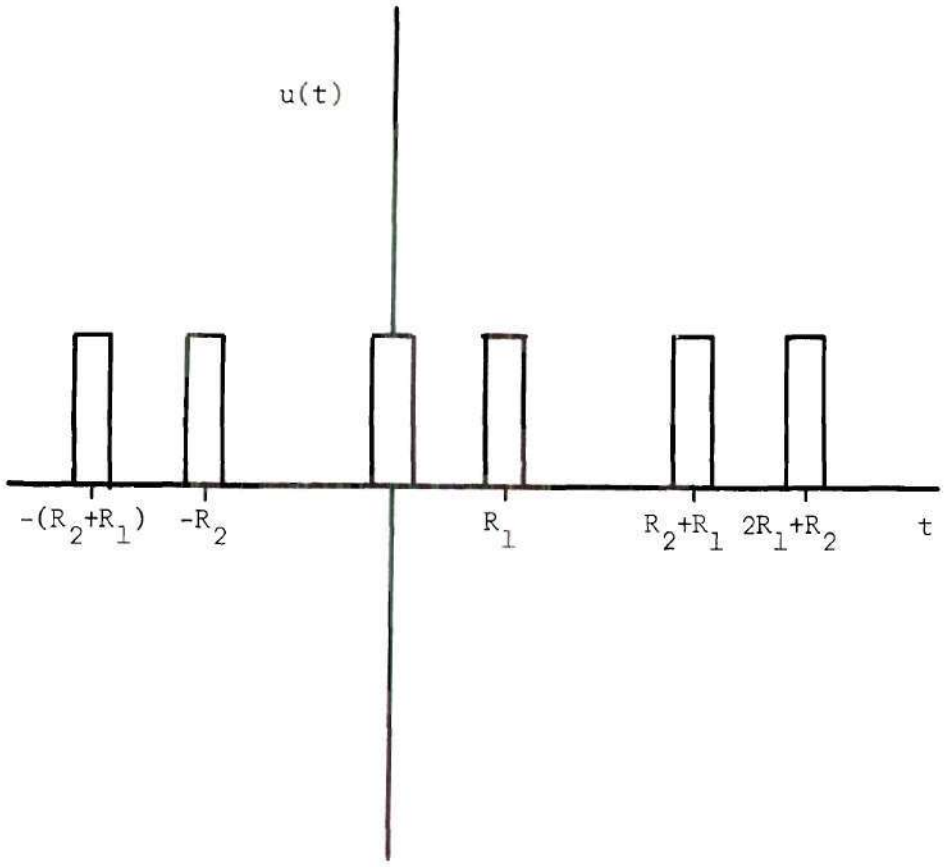


Figure 14. A Staggered Pulse Train Waveform

is assumed to contain two parallel channels (Figure 15), alternately selects the pulses. The outputs from channels one and two are shown in Figure 15.

The Fourier transform of the signal coming from channel one is

$$F_1(\omega) = \frac{2A}{\omega} e^{-jn(R_1+R_2)\omega} \tag{36}$$

and that coming from channel two is

$$F_2(\omega) = \frac{2A}{\omega} e^{-j\omega R_1} e^{-jn(R_1+R_2)\omega} . \tag{37}$$

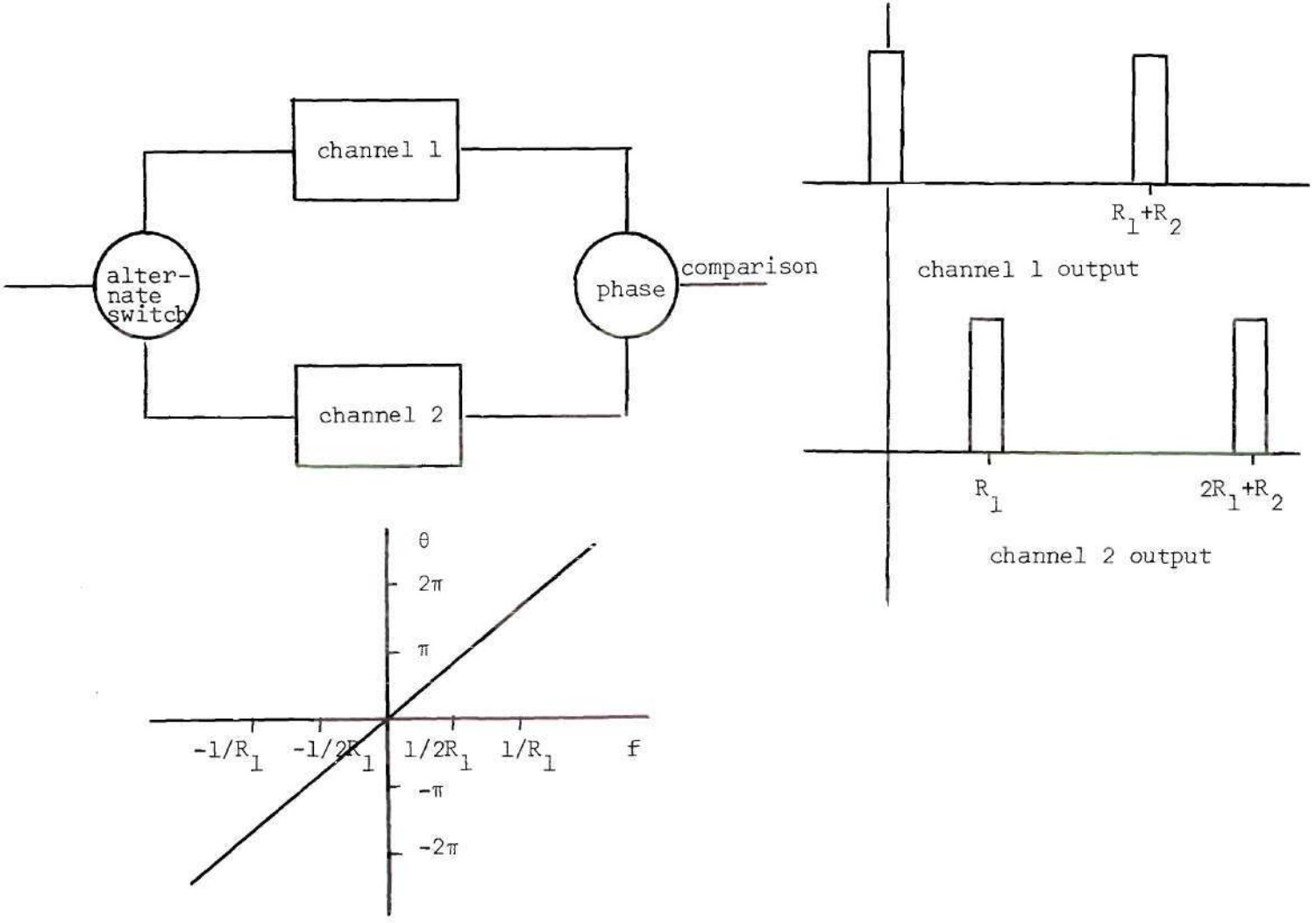


Figure 15. A Receiver Which Alternately Selects Pulses from a Staggered Pulse Train and its Outputs

Notice that $F_1(\omega)$ and $F_2(\omega)$ differ in phase by the factor $e^{-j\omega R_1}$. It is known that the Doppler ambiguities occur for $\omega = \frac{2\pi N}{T_r}$. Therefore, the Doppler ambiguities can be distinguished by comparing the phase between channels one and two and Doppler ambiguities can be resolved.

We may use the technique of H. H. Woerrlein to eliminate Doppler ambiguities while transmitting a shorter wavelength for increased Doppler resolution with a shorter length pulse train burst.

Consider the reduction in wavelength by a factor of ten. The shorter wavelength gives a corresponding reduction by a factor of ten of the number of pulses required in the burst. The transmitted waveform has the form shown in Figure 14. The outputs of channels one and two of the receiver differ in phase by $e^{-j\omega R_1}$. The Doppler ambiguities occur for $\omega = \frac{\pm 2\pi n}{T_r}$. The output of the channels differ in phase by

$$\theta_d = \pm \frac{2\pi n R_1}{T_r} . \tag{38}$$

With the new choice of wavelength there is a serious ambiguity inherent in the estimation of target velocity. There are now ten responses along the Doppler axis which can produce a return which could be confused with a target at rest. However, by setting $R_1 = \frac{T_r}{10}$, the phase between each ambiguous response is 18°. Undesired responses can now be eliminated by phase discrimination.

This receiver is more complex and requires parallel processing channels. However, the length of the pulse train required for the desired resolution properties has decreased from 268 to approximately

27 pulses and the total time duration of the waveform is 36 ms. There was a corresponding decrease in wavelength from 2.14 meters to 214 cm.

Theoretically, this phase discrimination technique could be used to further decrease the number of pulses required in the burst by transmitting a still shorter wavelength. The limit of this possible decrease occurs when the phase difference between the two channels can no longer be accurately estimated due to noise.

To avoid ambiguities due to repetition of the entire burst waveform, the repetition interval of the entire burst waveform should be equal to $NT_r$. Doppler ambiguities due to the repetition of the pulse train will then fall on the zeros of the ambiguity function.

The waveform design for the pulse train is now complete but there is an additional problem which must be considered if various size targets are present.

## Pulse Weighting

Notice in Figure 16 that the sidelobe levels for this train of five pulses are only -12.2 db below the central response peak. Thus, a target on one of these sidelobes with a cross section 12.2 db higher than that of the target appearing at $\tau = \phi = 0$ will produce a signal of equivalent magnitude. It would seem that the solution would be to decrease the magnitude of the ambiguity function between these large responses and hence have a greater possible dynamic range of targets. In a recent paper Rihaczek and Mitchell have considered this problem and formulated a solution to it (34). This solution will be summarized here.

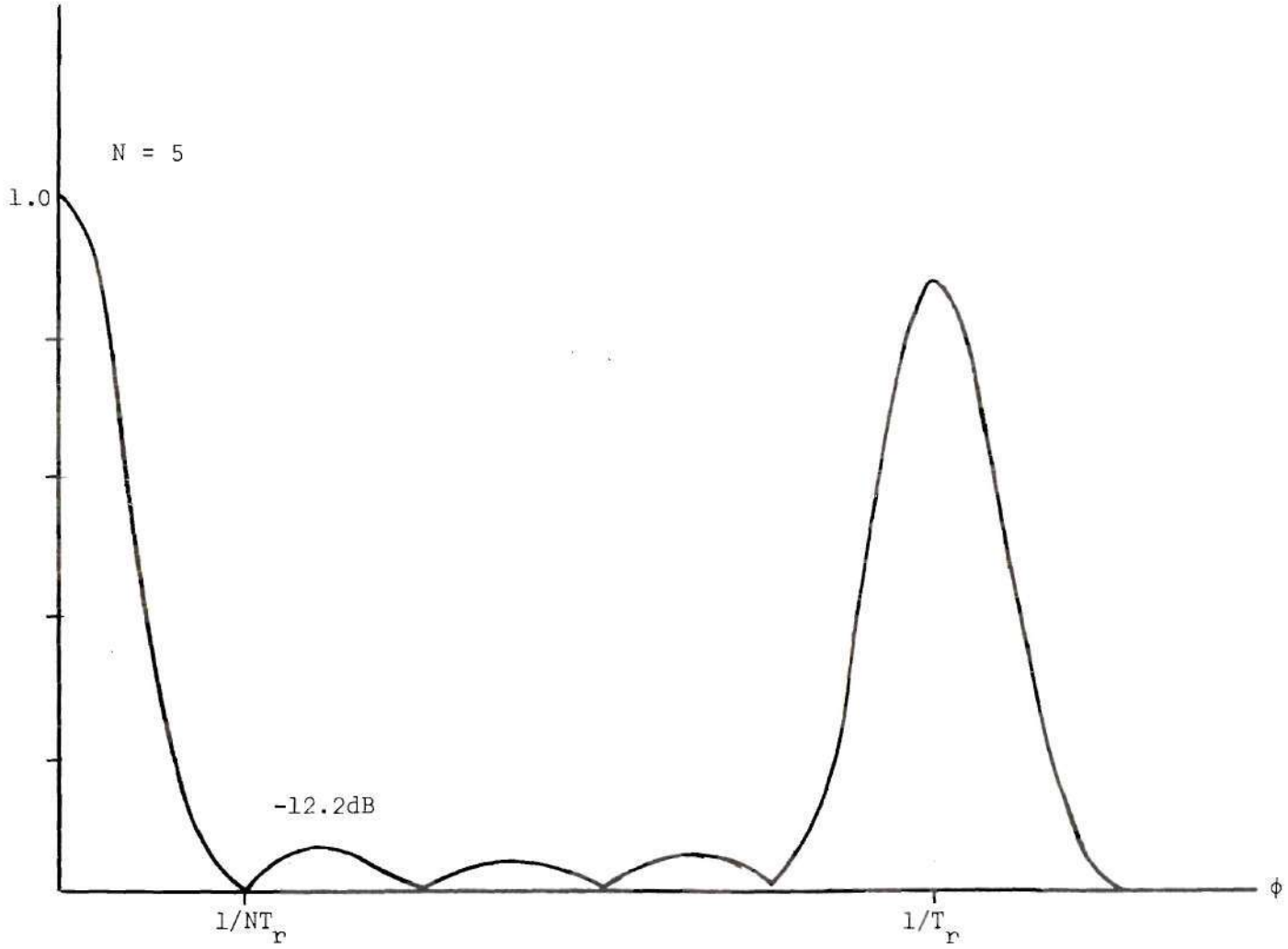


Figure 16. Ambiguity Function of the Uniform Pulse Train on the Doppler Axis

Let

$$u_1(t) = \sum_{n=0}^{N-1} a_n u_c(t-nT_r) \tag{39}$$

be the complex envelope of the received signal and

$$u_2(t) = \sum_{m=0}^{N-1} b_m u_c(t-mT_r) \tag{40}$$

be the waveform to which the receiver is matched. The weighting factors $a_n$ and $b_m$ are, in general, complex. The envelope function is

$$\psi(\tau,\phi) = \sum_{n=0}^{N-1} \sum_{m=0}^{N-1} a_n b_m^* e^{j2\pi\phi nT_r} \psi_c(\tau-[n-m]T_r,\phi) \tag{41}$$

where

$$\psi_c(\tau,\phi) = \int_{-\infty}^{\infty} u_c(t)u_c^*(t-\tau)e^{j2\pi\phi t}dt \tag{42}$$

is the envelope function of a component pulse. The terms centered at $\tau = pT_r$ can be collected by writing the double sum as

$$\sum_{n=0}^{N-1} \sum_{m=0}^{N-1} = \sum_{p=0}^{N-1} \sum_{m=0}^{N-1-p} \Bigg|_{n=m+p} + \sum_{p=-(N-1)}^{-1} \sum_{n=0}^{N-1-|p|} \Bigg|_{m=n-p} \tag{43}$$

Substituting this into Equation (41) and taking the duty cycle less than 50 per cent, we obtain

$$|\psi(\tau,\phi)| = \sum_{p=0}^{N-1} |\psi_c(\tau-pT_r,\phi)| \left| \sum_{m=0}^{N-1-p} a_m + pb_m^* e^{j2\pi\phi mT_r} \right| \tag{44}$$

$$+ \sum_{p=-(N-1)}^{-1} |\psi_c(\tau-pT_r,\phi)| \left| \sum_{m=0}^{N-1-|p|} a_m b_{m+|p|}^* e^{j2\pi\phi mT_r} \right|.$$

The ambiguity surface on the $\tau,\phi$ plane is thus represented by the sum of p surfaces centered at $\tau = pT_r$ on the delay axis. Our goal is the suppression of Doppler ambiguities by pulse train weighting and now the question is what type of weighting is needed.

From Equation (44) a given p surface is given by

$$|\psi_p(\tau,\phi)| = |\psi_c(\tau-pT_r,\phi)| \left| \sum_{m=0}^{N-1-p} a_{m+p} b_m^* e^{j2\pi\phi mT_r} \right|. \tag{45}$$

The inverse Fourier transform of the sum in Equation (45) is

$$F^{-1}\left\{ \sum_{m=0}^{N-1-p} a_{m+p} b_m^* e^{j2\pi\phi mT_r} \right\} = \sum_{m=0}^{N-1-p} a_{m+p} b_m^* \delta(t-mT_r) \tag{46}$$

where $\delta(t)$ is the Dirac delta function. Now we define a continuous function $a(t)$ such that sampling $a(t)$ at intervals $mT_r$ yields the coefficients $a_m$. We assume $a(t) = 0$ outside the time interval of the train. A weighting function $b(t)$ for generating the coefficients $b_m$ is similarly defined. Therefore,

$$\sum_{m=0}^{N-1-p} a_{m+p} b_m^* \delta(t-mT_r) = \sum_{m=-\infty}^{\infty} a(t+pT_r) b^*(t) \delta(t-mT_r). \tag{47}$$

Since a(t) and b(t) are zero outside the pulse train interval, the extension of the limits on the right side of Equation (46) is permissible.

Substitution of Equation (47) in Equation (46) gives

$$\sum_{m=0}^{N-1-P} a_{m+p} b_m^* e^{j2\pi\phi m T_r} = F\{a(t+pT_r)b^*(t)\} * \frac{1}{T_r} \sum_{m=-\infty}^{\infty} \delta(\phi - m/T_r) \qquad (48)$$

where the star denotes convolution. Looking at Equation (45), the ambiguity function of the pulse $\psi_c(\tau-pT_r,\phi)$ is multiplied by a function generated by repetition of $F\{a(t+pT_r)b^*(t)\}$ at intervals $1/T_r$. Therefore, if $F\{a(t+pT_r)b^*(t)\}$ has low sidelobes, then the ambiguity function of the pulse train will also have low sidelobes. We desired to decrease the area under the envelope of $a(t+pT_r)b^*(t)$ between the large Doppler responses. This area can be decreased only by the adjustment of the magnitudes of the weighting function. If the phase of either a(t) or b(t) is adjusted, the sidelobes can be shifted in position but their general level remains unchanged because the envelope area is unchanged.

Rihaczek and Mitchell have used this result to greatly increase the dynamic range capability of pulse train waveforms. The general conclusion is that the sidelobe levels in Doppler can be decreased by an appropriate amplitude weighting. Some results for both unilateral and bilateral Gaussian weightings are shown in Figure 17. It is important to remember that the volume which has been removed from between the large Doppler responses must be located elsewhere by the

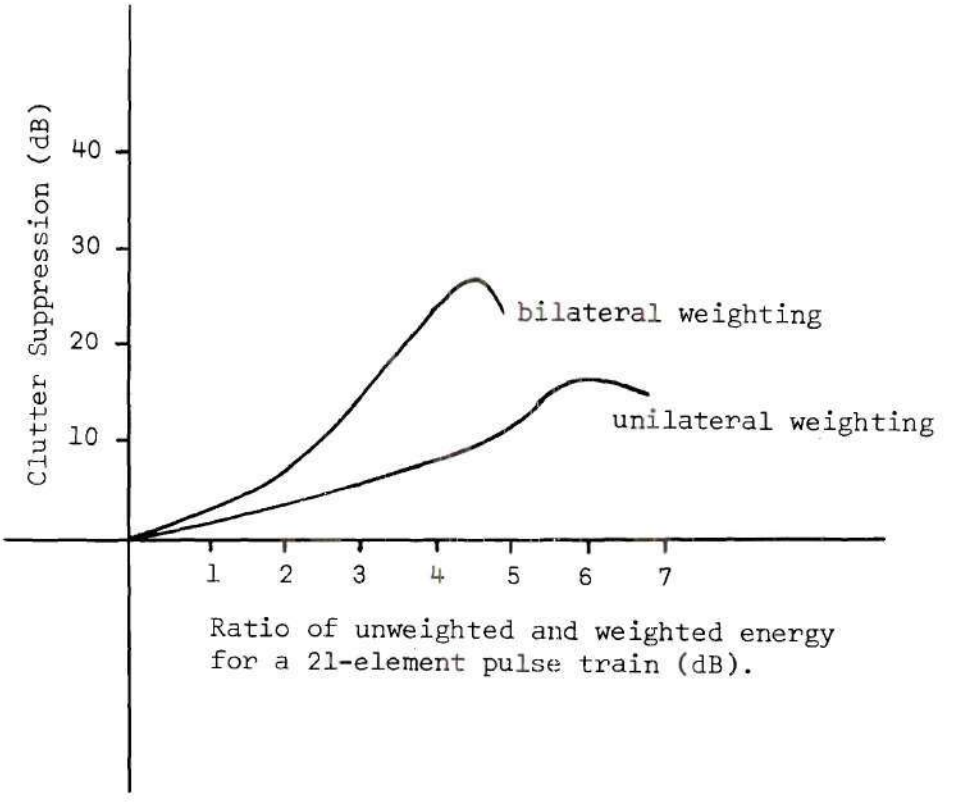


Figure 17. Clutter Suppression Properties of an Amplitude Weighted Pulse Train

volume constraint property. The additional volume will cause the large Doppler responses to increase slightly in width.

# CHAPTER V

## RESULTS

The radar ambiguity function has been treated with emphasis on its properties, limitations, and applications.

The properties form a set of necessary conditions which, with the exception of Property XII and Property X, all ambiguity functions must obey. They are, therefore, useful in checking to see if a given unknown function may be an ambiguity function. However, none of the properties is a sufficient condition. In addition, Properties I, II, III, IV, VI, VII, X, XI, and XII have applications in the graphing of ambiguity functions. Properties V and IX describe volume constraints which are not a function of waveform selection and which set definite bounds on the simultaneous resolution capabilities in Doppler and time delay of a radar.

The limitations treated are of two types:

(1) The ambiguity function cannot be applied to all waveforms because of the assumptions made in its derivation.

(2) Resolution limitations arise as a result of Properties V and IX.

The assumptions made in the derivation of the ambiguity function are

(1) The complex envelope representation of the transmitted signal is valid.

(2) The compression of the waveform due to its collision with a moving body can be accounted for by the Doppler shift.

(3) The ambiguity function assumes returns from point targets, i.e., the targets' dimensions are small when compared with the intrinsic resolution capability of the waveform.

(4) The approximation has been made that the effects of acceleration and all higher order range derivations can be ignored over the signal's time duration.

Property V states that all ambiguity functions have the same volume and only the volume distribution can be adjusted. Thus Property V places fundamental resolution limitations on a radar which operates in a dense, extended target environment. Property IX places limitations on the maximum clear area which may surround the central response peak of an ambiguity function.

Chapter IV deals with some applications of the ambiguity function. The ambiguity function is applied to waveform design and can be used to illustrate the resolution, accuracy, and ambiguity distribution of a waveform. Since target detection depends only on the signal energy transmitted, waveforms with very different ambiguity characteristics can have the same target detection probability. The clutter suppression techniques of Rummler, Blau, Rasmussen, Ares, Rihaczek, and Mitchell all use the ambiguity function. In addition, various ambiguity patterns were plotted for particular target environments. All of the most frequently used waveform types have been presented. Some three-dimensional plots of typical ambiguity functions are shown in Appendix II.

Since pulse trains readily lend themselves to use, emphasis has been placed on both range resolution trains and pulse trains for simultaneous resolution in velocity and range. A waveform design for a pulse train was presented and the techniques of H. H. Woerrlein and August Rihaczek were shown to be useful in eliminating "distal" ambiguities and sidelobe interference.

In all of the waveform examples for simultaneous resolution in velocity and range we have severely limited ourselves. An attempt has been made to simultaneously estimate these parameters after looking at the output of a matched filter for one waveform reflection. This constraint is artificial since targets do not suddenly appear or disappear, but have a history of position and velocity. The ambiguity function, however, is not a good model for taking a target's history into account. Further work in waveform design probably should be toward development of a model which includes target history.

# APPENDIX I

## DERIVATION OF THE AMBIGUITY FUNCTION

# APPENDIX I

## DERIVATION OF THE AMBIGUITY FUNCTION

The signal presented to the receiver is

$$S(t) = u(t-t')e^{j(\omega_o-\Omega')(t-t')} .$$

The signal has a time shift t' and a Doppler shift $\Omega'$.

The impulse response of a filter matched to a time shift t" and a Doppler shift $\Omega$" is

$$h(\tau) = u^*(-t"-\tau)e^{j(\omega_o-\Omega")(t"+\tau)} .$$

The response of the filter to an input S(t) is

$$e(t) = \int_{-\infty}^{\infty} S(\tau)h(t-\tau)d\tau$$

$$= \int_{-\infty}^{\infty} u(\tau-t')u^*(\tau-t-t")$$

$$e^{j\{(\omega_o-\Omega')(\tau-t')-(\omega_o-\Omega")(\tau-t-t")\}} d\tau .$$

Substitute $\eta + t' = \tau$

$$-\nu = t + t" - t'$$

$$e(t'-t''-\nu) = e^{-j\nu(\omega_o-\Omega'')} \int_{-\infty}^{\infty} u(\eta)u^*(\eta+\nu)e^{-j\eta 2\pi\phi}d\eta.$$

The envelope of this waveform is the quantity of interest.

$$\psi(\nu,\phi) = \int_{-\infty}^{\infty} u(\eta)u^*(\eta+\nu)e^{-j\eta 2\pi\phi}d\eta$$

Let $\nu = \tau$, $\eta = t$, and

$$\psi(\tau,\phi) = \int_{-\infty}^{\infty} u(t)u^*(t+\tau)e^{-j2\pi\phi t}dt.$$

The square of this envelope is the ambiguity function.

# APPENDIX II

## THREE-DIMENSIONAL PLOTS OF SOME TYPICAL AMBIGUITY FUNCTIONS

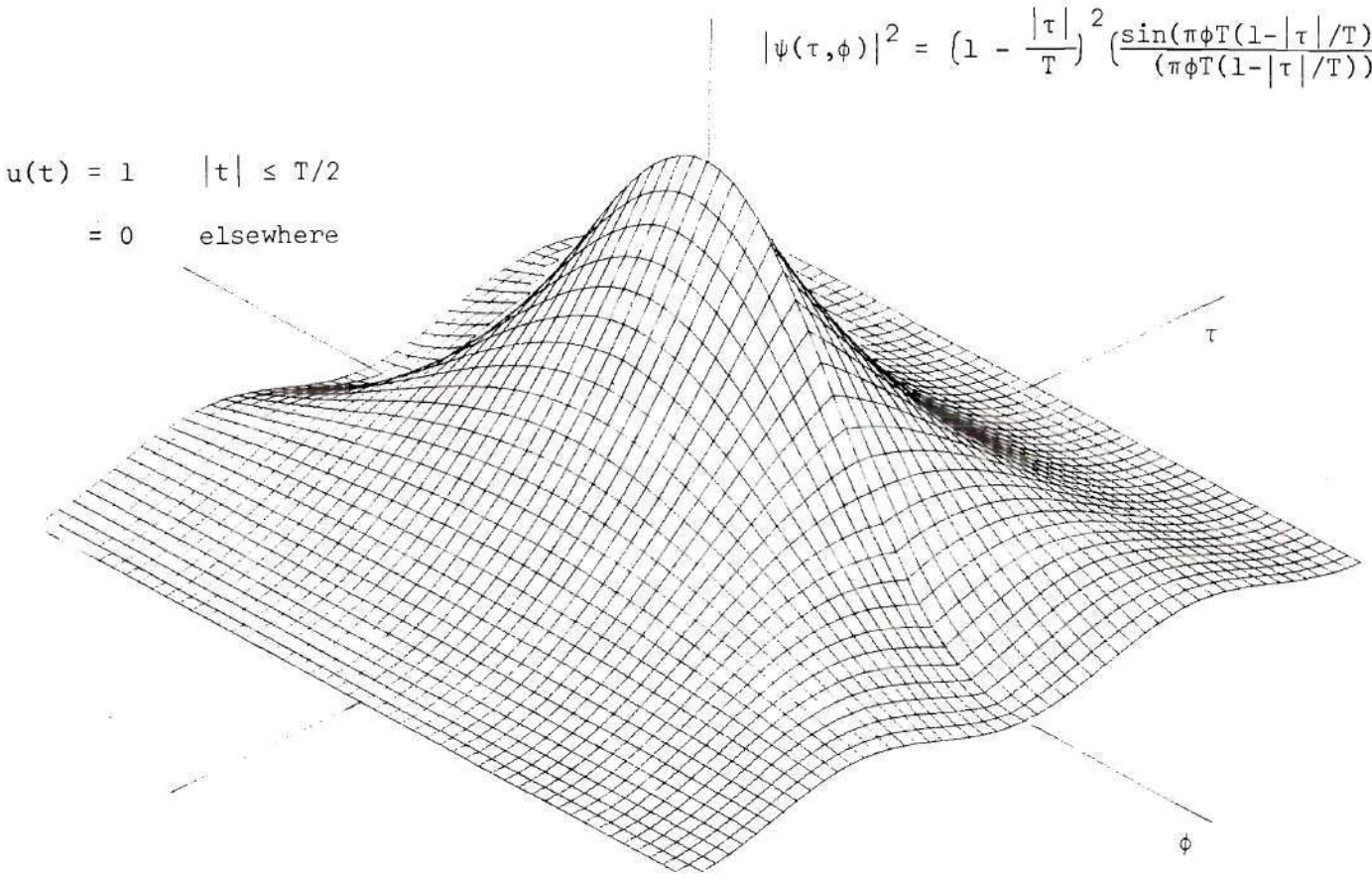


Figure 18. Ambiguity Function for a Pulse with Duration T

$$u(t) = 1 \quad |t+3T| < T/2,\ |t-3T| < T/2,\ |t| < T/2$$

$$= 0 \text{ elsewhere}$$

$$|\psi(\tau,\phi)|^2 = (1/3)^2 \frac{\sin^2 \pi\phi(T-\tau)}{(\pi\phi)^2} [1+2\cos 6\pi\phi T]^2$$

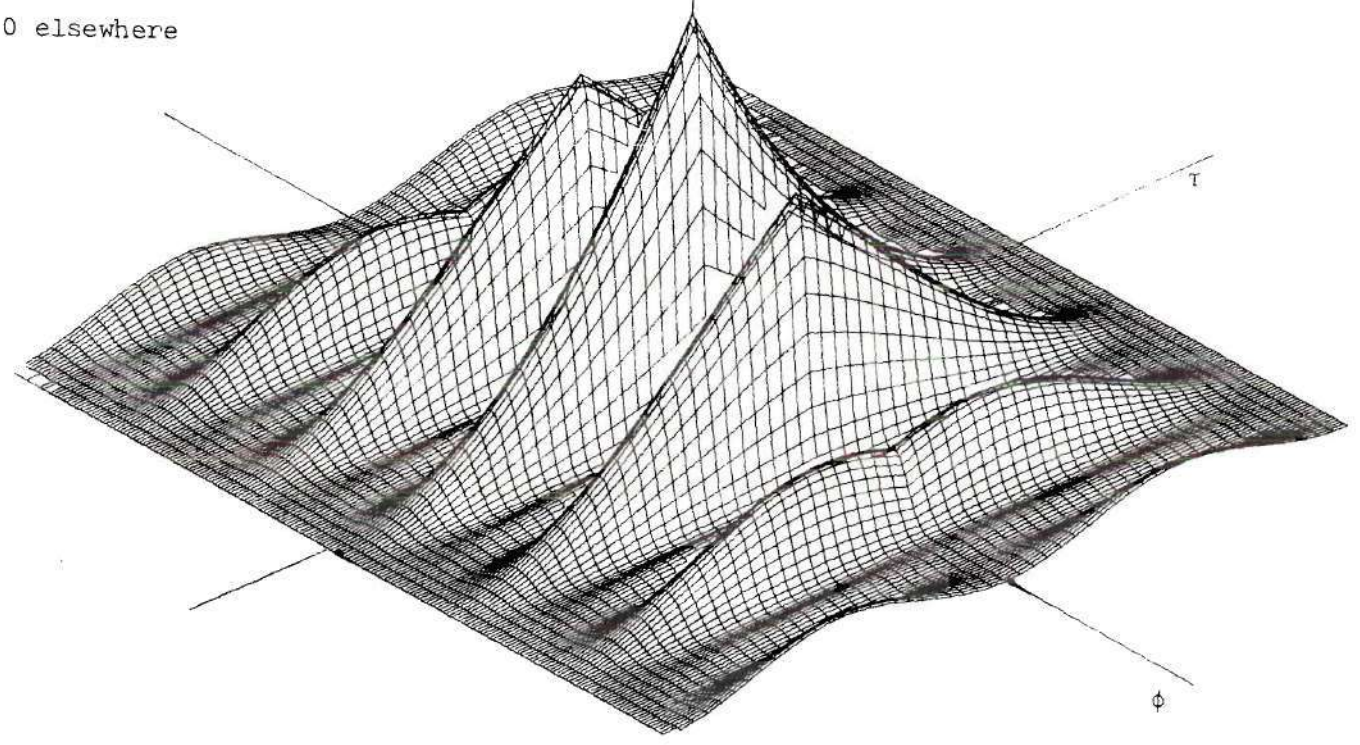


Figure 19. Ambiguity Function for a Three Pulse Train for $|\tau| \leq T$ and $|\phi| \leq 1/T$

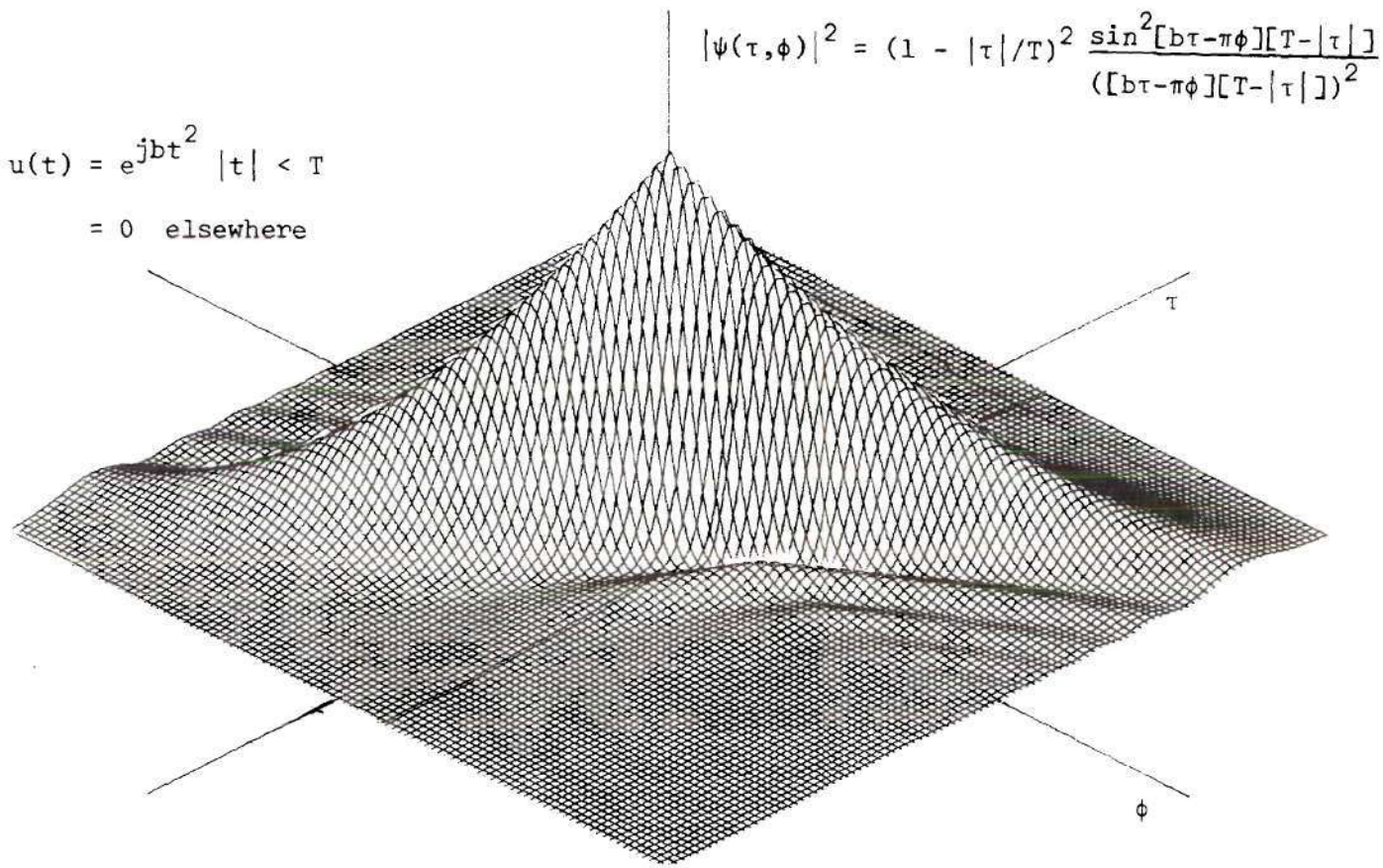


Figure 20. Ambiguity Function of a Linear FM Waveform with a Time Bandwidth Product of 25 for $|\tau| \leq T$ and $|\phi| \leq 5/T$

# BIBLIOGRAPHY

# BIBLIOGRAPHY


1. P. M. Woodward, "Probability and Information Theory with Applications to Radar," New York: Pergamon Press, 1953.

2. D. O. North, "An Analysis of the Factors which Determine Signal/Noise Discrimination in Pulsed-Carrier Systems," Proc. IEEE, Vol. 51, pt. 2, July 1963, pp. 1016-1027.

3. Charles E. Cook and Marvin Bernfield, "Radar Signals, An Introduction to Theory and Applications," New York: Academic Press, 1967, pp. 24-28.

4. P. M. Woodward and I. L. Davies, "A Theory of Radar Information," Philosophical Magazine, vol. 41, 1950, pp. 1001-1017.

5. W. M. Siebert, "Studies of Woodward's Uncertainty Function," MIT Research Laboratory of Electronics, Quarterly Progress Report, vol. 49, April 15, 1958, pp. 90-94.

6. E. C. Westerfield, R. H. Prager, and J. L. Stewart, "Processing Gains Against Reverberation (Clutter) Using Matched Filters," IRE Transactions on Information Theory, vol. IT-6, June 1960, pp. 204-218.

7. J. R. Klauder, "The Design of Radar Signals Having Both High Range Resolution and High Velocity Resolution," The Bell System Technical Journal, vol. 39, no. 4, July 1960, pp. 809-820.

8. C. W. Helstrom, "Statistical Theory of Signal Detection," New York: Pergamon Press, 1960, p. 21.

9. Ibid., p. 280.

10. D. Gabor, "Theory of Communication," The Journal of the Institute of Electrical Engineers, vol. 93, pt. 3, no. 21, January 1946, pp. 429-441.

11. E. J. Kelly and R. P. Wishner, "Matched-Filter Theory for High-Velocity, Accelerating Targets," IEEE Transactions on Military Electronics, vol. MIL-9, January 1965, pp. 56-69.

12. August W. Rihaczek, "Delay Doppler Ambiguity Function for Wide-Band Signals," IEEE Transactions on Aerospace and Electronic Systems, vol. AES-3, no. 4, July 1967, pp. 705-711.

13. William Blau, "Radar Partial Coherence Theory: An Introduction," IEEE Transactions on Aerospace and Electronic Systems, vol. AES-2, no. 5, September 1966, pp. 536-543.

14. H. Urkowitz, C. A. Hauer, and J. F. Koval, "Generalized Resolution in Radar Systems," Proceedings of the IRE, vol. 50, no. 10, October 1962, pp. 2093-2105.

15. Helstrom, pp. 231-237.

16. Ibid., p. 21.

17. Ibid., pp. 223-231.

18. August W. Rihaczek, "Radar Signal Design for Target Resolution," Proceedings of the IRE, vol. 53, no. 2, February 1965, pp. 116-128.

19. R. Price and E. M. Hofstetter, "Bounds on the Volume and Height Distributions of the Ambiguity Function," IEEE Transactions on Information Theory, vol. IT-11, no. 2, April 1965, pp. 207-214.

20. W. M. Siebert, "A Radar Detection Philosophy," IRE Transactions on Information Theory, vol. IT-2, pp. 204-221.

21. William D. Rummler, "A Technique for Improving the Clutter Performance of Coherent Pulse Train Signals," IEEE Transactions on Aerospace and Electronic Systems, vol. AES-3, no. 2, January 1967, pp. 139-141.

22. William Blau, "Synthesis of Ambiguity Functions for Prescribed Responses," IEEE Transactions on Aerospace and Electronic Systems, vol. AES-3, no. 4, July 1967, pp. 656-663.

23. Manuel Ares, "Optimum Burst Waveforms for Detection of Targets in Uniform Range--Extended Clutter," IEEE Transactions on Aerospace and Electronic Systems, vol. AES-3, no. 2, January 1967, pp. 139-141.

24. C. P. Rasmussen, "Clutter Rejection Using a Coded Burst Waveform," Eascon 1968 Convention Record, pp. 70-78.

25. August W. Rihaczek and Richard L. Mitchell, "Radar Waveforms for Suppression of Extended Clutter," IEEE Transactions on Aerospace and Electronic Systems, vol. AES-3, no. 3, May 1967, pp. 510-517.

26. R. H. Pettit, "Pulse Sequences with Good Autocorrelation Properties," Microwave Journal, vol. 10, no. 3, February 1967, pp. 63-67.

27. J. B. Resnick, "High Resolution Waveforms Suitable for a Multiple Target Environment," M.S. Thesis, Massachusetts Institute of Technology, Cambridge, Mass., June 1962.

28. C. E. Cook, "Pulse Compression--Key to More Efficient Radar Transmission," Proceedings of the IRE, vol. 48, pt. 1, March 1960, pp. 310-316.

29. J. R. Klauder, A. C. Price, S. Darlington, and W. J. Albersheim, "The Theory and Design of Chirp Radars," Bell System Technical Journal, vol. 39, July 1960, pp. 745-808.

30. Merrill I. Skolnik, Introduction to Radar Systems, New York: McGraw Hill Book Company, 1962, p. 468.

31. A. W. Rihaczek and R. L. Mitchell, "Matched Filter Responses of the Linear FM Waveform," IEEE Transactions on Aerospace and Electronic Systems, vol. AES-4, no. 3, May 1968, pp. 417-432.

32. A. W. Rihaczek, "Radar Resolution Properties of Pulse Trains," Proceeding of the IRE, vol. 52, pt. 2, February 1964, pp. 153-164.

33. H. H. Woerrlein, "Eliminating Radar Ambiguities by Processing Staggered Pulse Trains or Spectra," Naval Research Laboratory Report, no. NRL-6651, February 19, 1968, AD 667455.

34. A. W. Rihaczek and R. L. Mitchell, "Clutter Suppression Properties of Weighted Pulse Trains," Aerospace Corporation Report, no. TR-0158 (3230-46)-9, February 1968, AD 668441.